

Copyright Warning & Restrictions

The copyright law of the United States (Title 17, United States Code) governs the making of photocopies or other reproductions of copyrighted material.

Under certain conditions specified in the law, libraries and archives are authorized to furnish a photocopy or other reproduction. One of these specified conditions is that the photocopy or reproduction is not to be “used for any purpose other than private study, scholarship, or research.” If a user makes a request for, or later uses, a photocopy or reproduction for purposes in excess of “fair use” that user may be liable for copyright infringement,

This institution reserves the right to refuse to accept a copying order if, in its judgment, fulfillment of the order would involve violation of copyright law.

Please Note: The author retains the copyright while the New Jersey Institute of Technology reserves the right to distribute this thesis or dissertation

Printing note: If you do not wish to print this page, then select “Pages from: first page # to: last page #” on the print dialog screen

The Van Houten library has removed some of the personal information and all signatures from the approval page and biographical sketches of theses and dissertations in order to protect the identity of NJIT graduates and faculty.

ABSTRACT
A Study of
Annular Slurry Jet for
Abrasive Waterjet Cutting

by
Thomas Kuriakose

The objective of this project is to study the performance of an annualr slurry jet nozzle for abrasive waterjet cutting. This nozzle has been invented by Avraham Harnoy, Department of Mechanical Engineering, NJIT and presented to the patent committee of NJIT in May 1990. This study includes design and development of prototydes and testing of their performance. Moreover, it includes initial theoretical study of the flow behavior.

The idea is based on the merging of a high velocity pure waterjet with an annular jet of a slurry of water and abrasives at low velocity. The two jets merge outside the nozzle. In this way, the major problems of wear and particle disintegration associated with conventional abrasive waterjet systems are eliminated. Our tests shows that it is possible to merge the two jets and the abrasive particles are accelerated. However, more experiments are required in actual cutting inorder to evaluate the merits of the proposed nozzle. Initial flow analysis helped to elucidate the flow pattern of the merging. More work is required to varify these results.

*The reason for confidentiality is that NJIT would like to retain the sole right for future technology transfer.

CONFIDENTIAL

**A STUDY OF
ANNULAR SLURRY JET FOR
ABRASIVE WATERJET CUTTING**

by
Thomas Kuriakose

A Thesis
Submitted to the Faculty of
New Jersey Institute of Technology
in Partial Fulfillment of the Requirements for the Degree of
Master of Science in Manufacturing Engineering
October, 1992

APPROVAL PAGE

A Study of Annular Slurry Jet for Abrasive Waterjet Cutting.

**by
Thomas Kuriakose**

Dr. Avraham Harnoy, Thesis Advisor
Associate Professor of Mechanical Engineering, NJIT

Dr. Ernest S. Geskin, Committee Member
Professor of Mechanical Engineering, NJIT

Dr. Steve Kotefski, Committee Member
Assistant Professor and Program Coordinator of Manufacturing
Engineering Technology, NJIT

BIOGRAPHICAL SKETCH

Author: Thomas Kuriakose

Degree: Master of Science in Manufacturing Engineering

Date: October, 1992

Undergraduate and Graduate Education:

- Master of Science in Manufacturing Engineering, New Jersey Institute of Technology, Newark, NJ, 1992
- Bachelor of Technology in Naval Architecture and Ship Building, Cochin University of Science and Technology, Cochin, India, 1989

Major: Manufacturing Engineering

Dedicated to Paul Zeno and Biju Dennis

ACKNOWLEDGMENT

I wish to express my sincere gratitude to Dr. Avraham Harnoy, my thesis adviser, for his guidance and timely help throughout the course of this work.

I am grateful to Dr. Ernest S. Geskin and Dr. Steve Kotefski who reviewed the work and helped me with constructive suggestions.

I am thankful to Mr. Leonid Tismenetskiy of Waterjet Research Lab for his help during the experiments.

Finally, special thanks to my colleagues Ekramul H. Khan and Ashok Avadhani for their valuable support and friendship.

TABLE OF CONTENTS

	Page
1 INTRODUCTION	1
1.1 Objective	1
1.2 Motivation	1
1.2.1 Conventional Nozzle	1
1.2.2 Need for Improvement	3
1.2.3 Annular Jet Principle	3
1.3 Scope of the Research	5
1.3.1 Preliminary Tests to Establish the Feasibility of the New Design.. ..	5
1.3.2 Theoretical Investigation of the Mixing Process	5
2 BACKGROUND OF AWJ CUTTING	7
2.1 Technology with Waterjet Cutting	7
2.2 Abrasive Water Jet (AWJ) Cutting	7
2.3 Advantages of AWJ Systems	7
2.4 Existing Abrasive Waterjet Systems	8
3 PROBLEMS IN THE EXISTING AWJ SYSTEMS	13
3.1 General	13
3.2 Excessive Wear of Slurry Nozzle	13
3.3 Disintegration of Abrasive Particles	15
3.3.1 Results	16
3.3.2 Factors Influencing the Disintegration	16

4 THE PROPOSED DESIGN	19
4.1 General Principle	19
4.2 Design Procedure	19
4.3 Stage 1: Design for Low Pressure.....	19
4.3.1 Nozzle	21
4.3.2 Mixing Tube	21
4.3.3 Adjustment of Abrasive Flow	23
4.3.4 Experiment Setup	23
4.3.5 Operation	23
4.4 Stage 2: Design and Development for High Pressure	25
4.4.1 Strength Calculation for the Inner Cylinder	28
4.4.2 Experiment Setup.....	29
4.4.3 Abrasive Feed	30
4.4.4 Operation.....	30
4.4.5 Results	30
4.4.6 Conclusions	31
5 FLOW SIMULATION	33
5.1 General	33
5.2 FIDAP fluid dynamics analysis package	33
5.3 FIDAP Structure.....	34
5.3.1 Pre- processor (FIPREP module)	34
5.3.2 Processor (FIDAP Module)	34
5.3.3 Post-processor (FIPOST Module)	34
5.4 Modeling of Turbulence	35
5.4.1 Mixing Length Model	35

5.4.2 k - ϵ Model	36
5.5 Solution Procedure	36
5.5.1 Problem Definition	36
5.5.2 Definition of Geometry	37
5.5.3 Non-dimensionalization of Geometry	39
5.6 Boundary Conditions	39
5.6.1 Velocity	39
5.6.2 Turbulent Kinetic energy k	41
5.6.3 Turbulent Dissipation ϵ	41
5.6.4 Viscosity	41
5.7 Initial Conditions	42
5.8 Free Surface Boundary	43
5.8.1 Two Stage Approach for Solution	43
5.9 Mesh Generation	43
5.10 Solution	44
6 RESULTS AND CONCLUSIONS	48
6.1 Velocity Distribution	48
6.2 Mixing Characteristics	49
APPENDIX	56
A DETAILED DRAWING OF THE ANNUALR SLURRY JET NOZZLE	56
B FIDAP INPUT FILE FOR INITIAL SOLUTION	57
C FIDAP INPUT FILE FOR FINAL SOLUTION	60
REFERENCES	63

LIST OF FIGURES

Figure	Page
1.1 Conventional AWJ Nozzle	2
1.2 Principle of Annular jet	4
2.1 Sand Blasting Apparatus	9
2.2 Guns for Forming Jets of Particulate Material	11
2.3 Wet Abrasion Blasting	12
3.1 Nozzle Diameter Vs. Time	14
3.2 Abrasive Disintegration During Ejection	17
4.1 Preliminary Design for Low Pressure	20
4.2 Mixing Tube	22
4.3 Experiment Setup for Preliminary Model	24
4.4 Nozzle Assembly for High Pressure	26
4.5 Solid Model of the Nozzle Assembly	27
4.6 Critical Region of Inner Cylinder	28
5.1 Flow Domain	37
5.2 Definition of Geometry	38
5.3 Boundary Conditions	40
5.4 Initial Mesh for Trial Solution	45
5.5 Deformed Mesh After Final Solution	46
6.1 Velocity Vector Plot	50
6.2 Velocity of a Particle Moving Along the Axis of the Jet	51
6.3 Velocity Profile of the Abrasive Jet at Various Stand off distances	52
6.4 Velocity Contour Plot	53
6.5 Trajectory of a Typical Particle in the Abrasive Stream	54
6.6 Streamline Contour Plot	55

CHAPTER 1

INTRODUCTION

1.1 Objective

The objective of this research is to experiment a new type of nozzle for abrasive waterjet cutting. The new design is based on annular jet principle, in which abrasive particles and high velocity waterjet are mixed outside the nozzle. Annular jet principle is an original invention by Harnoy which was presented to the patent committee of NJIT in May, 1990. The new design is aimed at minimizing the problems associated with the existing abrasive waterjet nozzle.

1.2 Motivation

The concept of abrasive waterjet (AWJ) has found extensive applications such as conventional machining, cleaning and surface finishing, rock cutting, mining, drilling and deep water cutting for offshore operations. Machining of hard materials is one of the challenging tasks effectively handled by AWJ systems. Depending on the application, the arrangement for abrasive entrainment varies in different AWJ systems.

1.2.1 Conventional Nozzle

The AWJ nozzle most widely used for machining applications is based on the design by Hashish, Kirby and Pao (1987). Figure 1.1 illustrates nozzle assembly. By entraining abrasive particles into a high velocity jet of liquid, an abrasive jet is created which can cut hard materials. A high velocity jet is produced by charging fluid under high pressure (5000 to 100,000 psi) through an orifice (diameter 0.001 to 0.050") of synthetic sapphire. The jet is directed through chamber where abrasive particles of

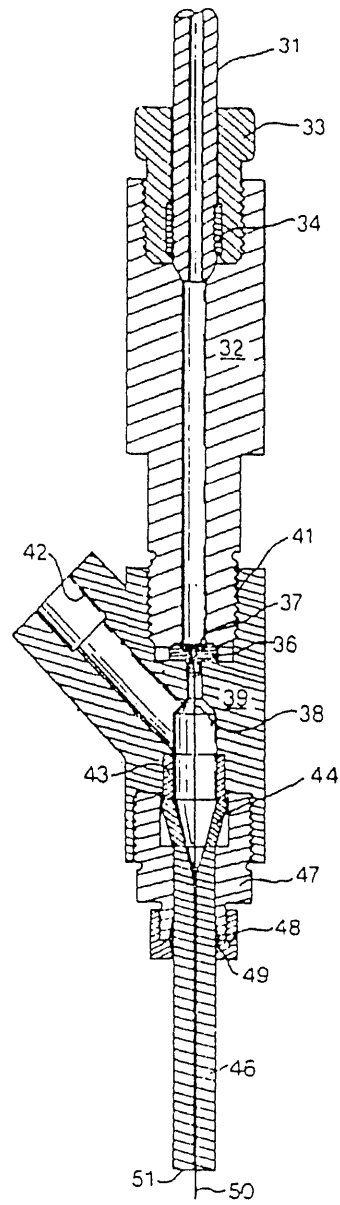


Figure 1.1 Conventional AWJ Nozzle.

low velocity are added. The partial vacuum created by the jet absorbs abrasives into the chamber. The converging section of the mixing tube (slurry nozzle) receives the jet and abrasives. The friction of the wall of slurry nozzle creates a low velocity boundary layer. The flow velocity will be much higher along the axis of the tube. As a result of this velocity gradient, the abrasive particles concentrate at the center of the jet.

1.2.2 Need for Improvement

Although this arrangement is capable of accelerating abrasive particles, there exists certain limitations. The inherent problems such as excessive nozzle wear and particle disintegration associated with this nozzle are discussed in chapter 3. The development of the new nozzle is motivated by the existing potential for a better abrasive entrainment mechanism which can minimize these problems.

1.2.3 Annular Jet Principle

As mentioned above, the proposed design is based on the principle of annular jet. Figure 1.2 illustrates the annular jet principle. A central, high velocity waterjet and another annular, low velocity abrasive slurry jet are merged outside the nozzle to form the abrasive waterjet. Although the concept of annular jet has been available before, its applications are limited to sand blasting and similar operations. The feasibility of utilizing annular jet for machining is investigated.

The formation of the high velocity waterjet is similar to the arrangement in conventional nozzle. Low pressure water and abrasives are pre-mixed to form an abrasive slurry. The annular jet is formed by introducing low pressure abrasive slurry into the annular cavity so that the slurry exits through the annular slit at the bottom of the cavity. The high velocity waterjet accelerates the abrasive particles to enable the cutting. The design procedure and operation of nozzle are described in chapter 4.

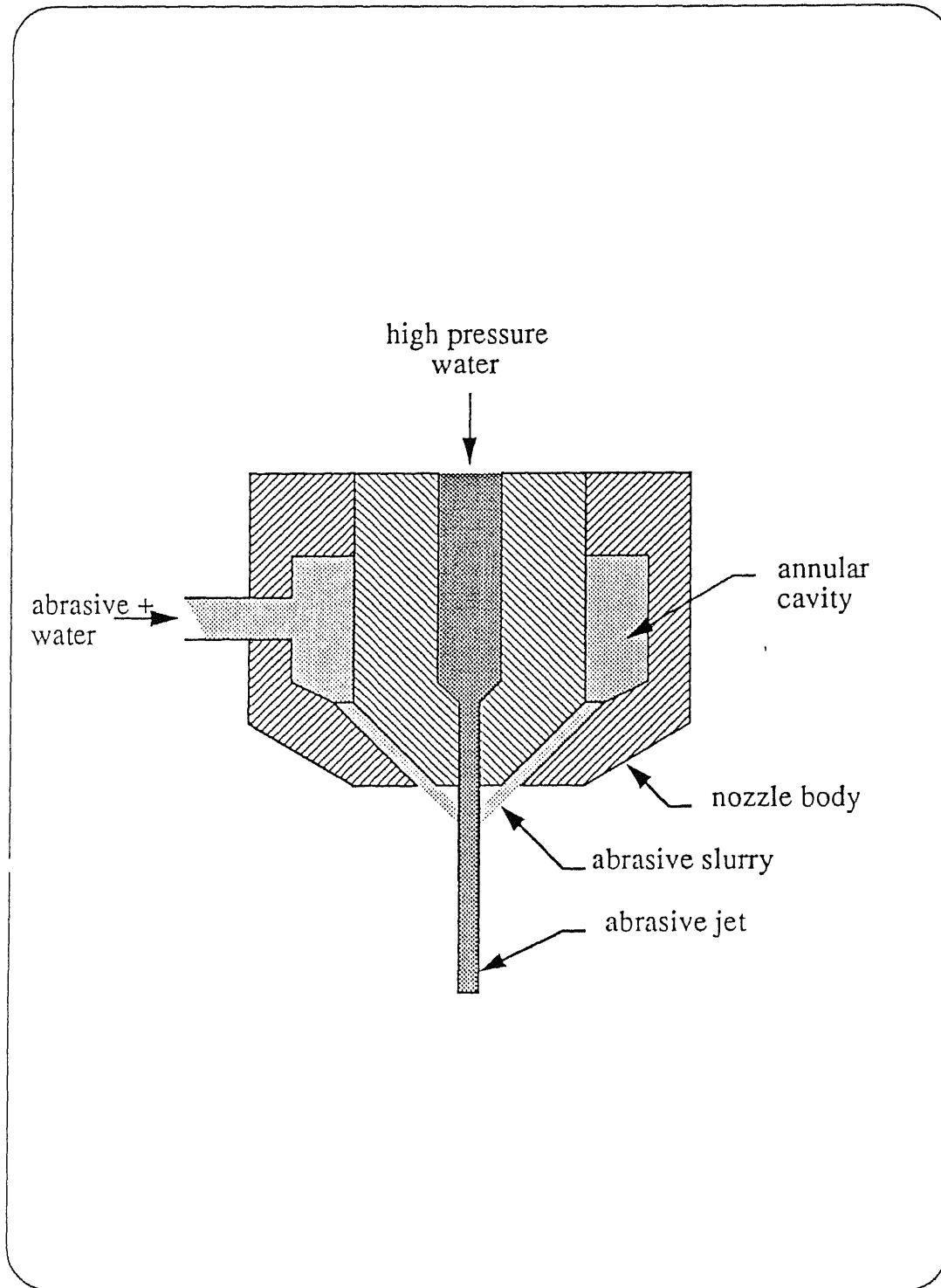


Figure 1.2 Principle of Annular jet.

Since abrasives are not accelerated inside the nozzle, wear of the nozzle due to erosion is minimal. Also, by eliminating the slurry nozzle, the disintegration of abrasive particles during the ejection process is virtually eliminated.

1.3 Scope of the Research

The current work had been focussed on two areas: (1) Preliminary tests to establish the feasibility of the new design and (2) Theoretical investigation of the mixing process.

1.3.1 Preliminary Tests to Establish the Feasibility of the New Design

This involved development of a prototype nozzle and conducting preliminary experiments to verify the principle of the annular jet. The objective of the experiments was to make sure that the high velocity jet and abrasive slurry merge, the abrasives are accelerated and the jet can perform the cutting.

The development of the prototype nozzle was done in two stages. In the first stage, a preliminary model was developed for testing in low pressure. Tests were conducted using supply water at 60 psi. to verify the abrasive feed mechanism and to study the merging of the jets.

Based on the results of first stage, prototype nozzle for high pressure was developed in the second stage. Preliminary experiments were conducted in the waterjet cutting machine to evaluate the performance. The design procedure, experiments and the results are discussed in chapter 4.

1.3.2 Theoretical Investigation of the Mixing Process

The flow of high velocity waterjet is essentially turbulent. Turbulence is a complex process involving random and three dimensional motion. Though the exact prediction of turbulent flow is nearly impossible, several numerical methods are available which

give reasonably good prediction of the turbulent phenomena. Based on the results of theoretical simulation, optimum design of the nozzle can be carried out.

Mixing of abrasive slurry with the high velocity jet and acceleration of the abrasives are the key processes in the AWJ formation. A numerical model based on Finite Element Method (FEM) was used for the analysis of AWJ flow. The solution procedure is outlined in chapter 5. The results are discussed in chapter 6.

CHAPTER 2

BACKGROUND OF AWJ CUTTING

2.1 Technology with Waterjet Cutting

Waterjet cutting (WJC) involves the removal of material by directing a thin, high velocity jet of water to the work piece. Pure Waterjet can efficiently cut a variety of materials such as corrugated box board, paper, plastics, leathers, asbestos, circuit boards etc. The first commercial WJC system was developed for the use in paper industry by McCartney Manufacturing Co., a division of Ingersoll-Rand Co. in late 1971.

2.2 Abrasive Water Jet (AWJ) Cutting

Pure water jet is not capable of cutting harder materials. Mixing of abrasive particles with the high velocity water jet is an excellent way to increase the cutting capabilities of water jets. This is called Abrasive waterjet (AWJ) cutting. Abrasive Waterjet can cut harder materials which include super alloys, composites, titanium, ceramics, carbon and stainless steel, glass and concrete. Although Water jet cutting technique is one of the recently introduced machining methods, it has found extensive applications in the industry. Applications of Waterjet technology is not limited to conventional machining processes. WJC has become a versatile tool for many applications such as rock cutting, mining, drilling and deep water cutting for offshore operations. In medical field, use of water jet for surgery is at its beginning.

2.3 Advantages of AWJ Systems

Compared to conventional cutting processes, abrasive waterjet cutting has many advantages. They are capable of cutting almost any material. There is negligible heat

build up and deformation stresses on the machined part as with laser electron beam and plasma arc cutting. No potential fire hazard is associated with the cutting process. There is considerable material savings because of reduced kerf and closer parts spacing. Also they provide exceptional surface quality, high material removal rates and omni-directional machining that makes this method ideal for automation (Kovacevic 1990). Since the process is omni-directional, contours, shapes and bevels of any angle can be accurately cut. In conventional machining processes, the tool and work piece are in contact which results in significant tool wear. Where as in WJ cutting, there is no direct contact between the tool and work piece, eliminating the sharpening requirements and hence the process can be more accurate. AWJ systems are easily adaptable to remote operations and control. When used with CNC, any changes in cutting pattern is easily accommodated and hence used extensively in Flexible Manufacturing Systems (FMS).

2.4 Existing Abrasive Waterjet Systems

As mentioned above, in AWJ cutting, abrasive particles are entrained into pure waterjet for cutting harder materials. There are several approaches for producing abrasive waterjets. Basically, these approaches can be classified into two groups, depending on whether the abrasives are mixed downstream or upstream of the high pressure nozzle.

2.4.1 High Velocity Abrasive Jet for Machining

The most commonly used AWJ nozzle for machining is based on the design by Hashish, Kirby and Pao (1987). The operation of this nozzle is described in chapter 1. The nozzle assembly is illustrated in figure 1.1.

Examples of the AWJ nozzles used for applications such as sand blasting and industrial cleaning are discussed below.

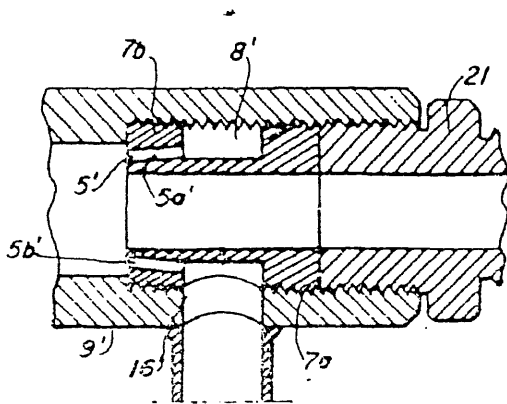
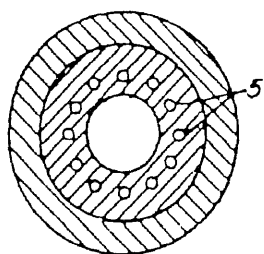
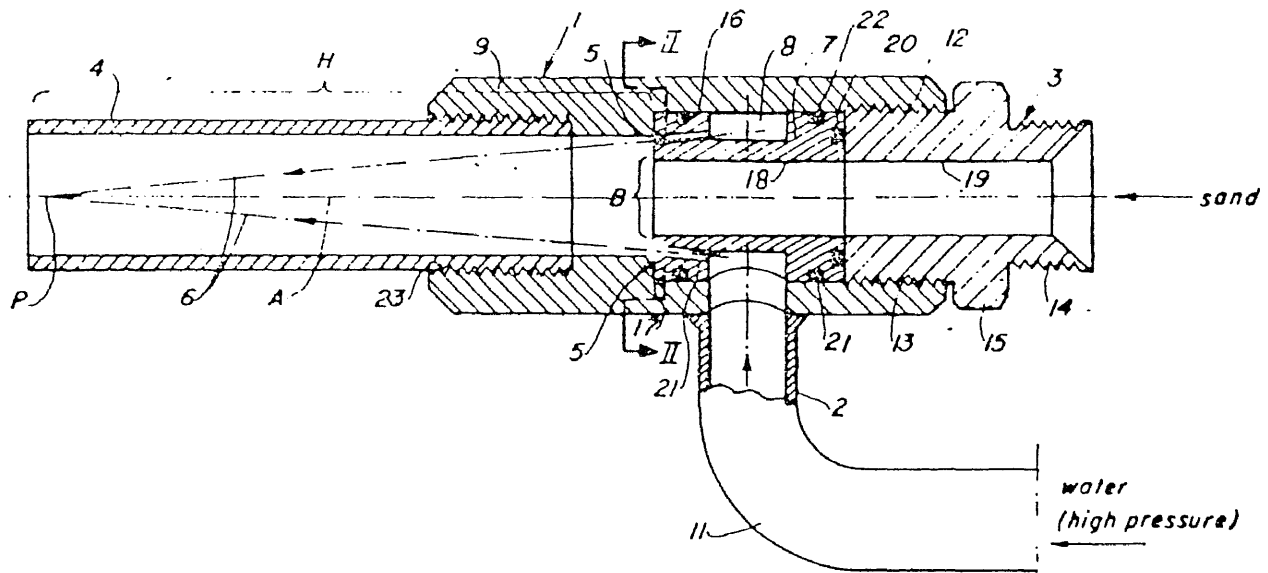


Figure 2.1 Sand Blasting Apparatus.

2.4.2 Sand Blasting Apparatus

Figure 2.1 illustrates the configuration of this nozzle developed by Maasberg and Sparkel (1969). A stream of granular material, typically sand, is passed through a tubular nozzle and water at pressure above 50 atmospheres is directed towards this granular stream. Water forms a coaxial convergent jet which mix with the granules and accelerates them. Typical application of this nozzle is sand blasting.

2.4.3 Guns for forming Jets of Particulate Material

This is an invention of Hart (1976). Figure 2.2 shows the nozzle assembly. Slurry jet in the middle is mixed with waterjets from the sides to form a high energy cleaning sheet of slurry. Typical applications of this system are cleaning buildings and ship hulls.

2.4.4 Wet Abrasion Blasting

This nozzle is developed by Easton (1978). The abrasive particles used are soluble in water and in this method problem of disposal of abrasive residue is eliminated. Figure 2.3 illustrates the nozzle assembly.

The abrasives are fed through the central orifice and multiple converging jets of high pressure water act as carrier for the abrasives. Typical abrasive material used is powdered sodium silicate, either alone or in admixture with common salt.

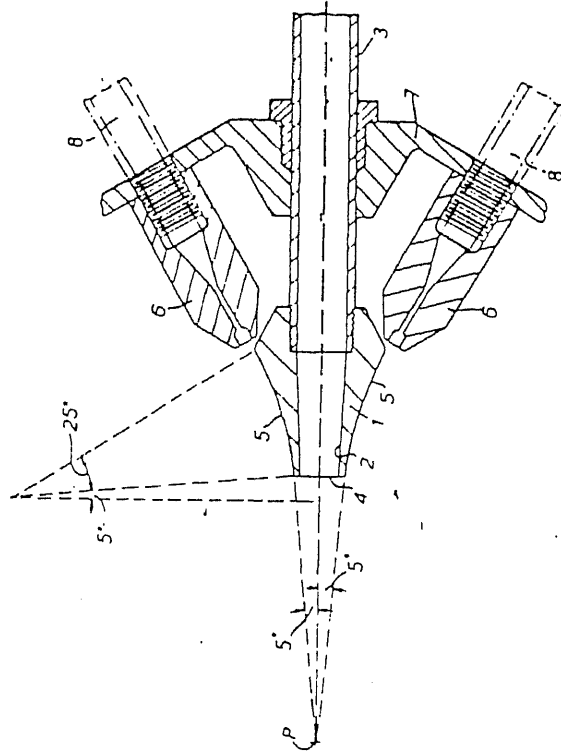


Figure 2.2 Guns for Forming Jets of Particulate Material.

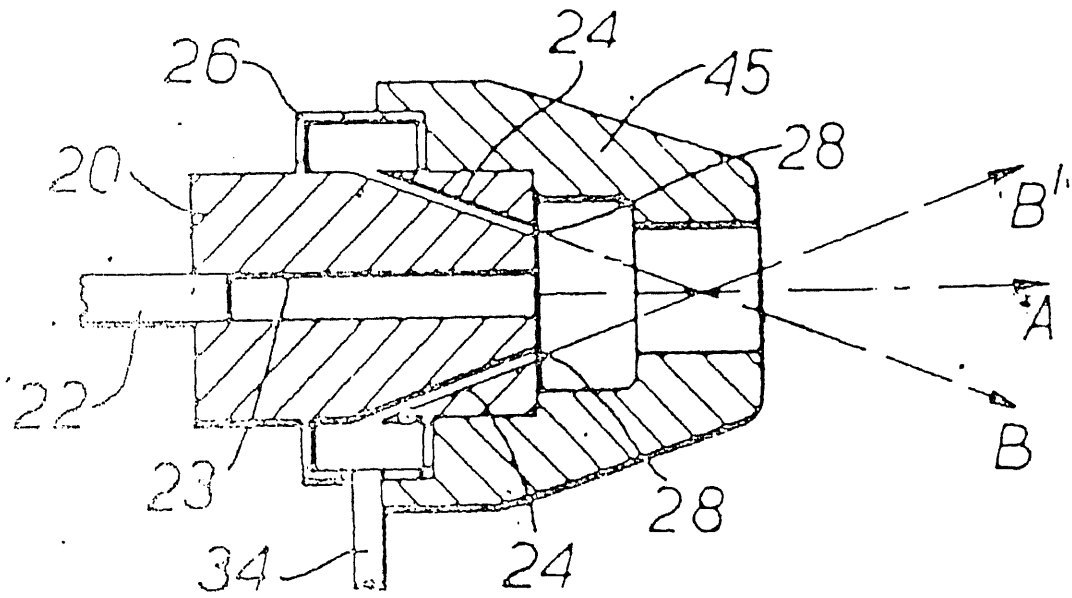


Figure 2.3 Wet Abrasion Blasting.

CHAPTER 3

PROBLEMS IN THE CONVENTIONAL AWJ SYSTEM

3.1 General

AWJ nozzle is one of the key parts in an AWJ system and hence the performance of the AWJ nozzle is critical to the overall technical and economical performance of the system.

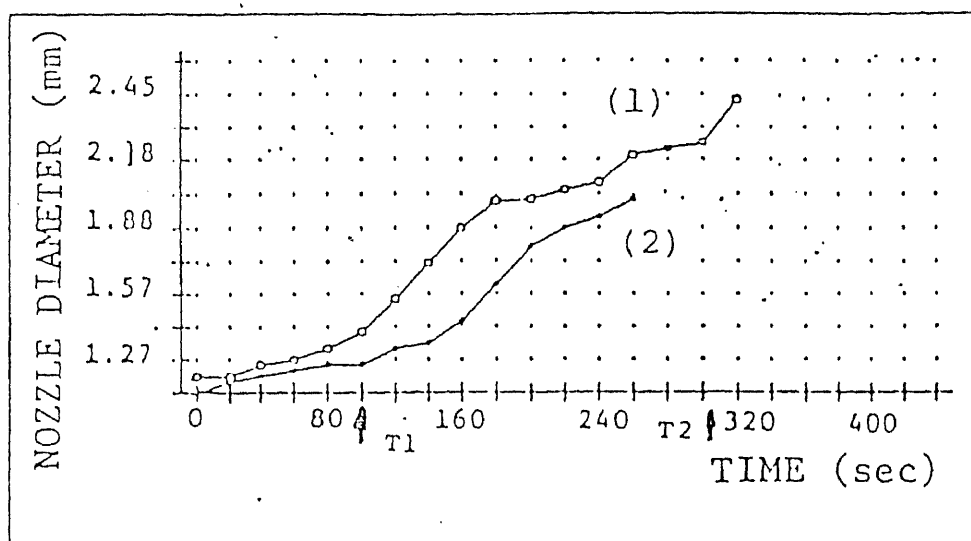
In most AWJ systems for machining, abrasives and water are mixed prior to accelerating through the slurry nozzle. Although these systems are very effective, some inherent problems exist in the abrasive entrainment mechanism which limit their performance.

3.2 Excessive Wear of Slurry Nozzle

AWJ process is essentially an erosion process that depends on the nature of the eroded and abrasive materials and on the velocity of the abrasive particles. This means that during operation, AWJ nozzle is subjected to abrasive and erosive modes of wear.

In the conventional AWJ system, the high speed water jet emanating from the sapphire nozzle creates vacuum which absorb the abrasive particles introduced from side. The converging section of the AWJ nozzle receive the mixture which is then accelerated through the tube. At the entrance, the impact of abrasives in the AWJ nozzle is at random angles. But as the flow proceeds through the tube, the abrasive particles travel parallel to the wall. This causes either abrasion or shallow impact erosion.

The nozzle wear depends on several parameters like pressure, jet velocity, size and type of abrasives, geometry and material of nozzle etc. The velocity of the abrasive mixture passing through the nozzle is of the order of 700 m/sec. Results of experiments to study the influence of waterjet pressure and abrasive flow rate on AWJ nozzle wear



(2) $P = 207$ MPa, $Q = 0.453$ kg/min

(1) $P = 262$ MPa, $Q = 0.453$ kg/min

Figure 3.1 Nozzle Diameter Vs. Time.

showed that an increase of waterjet pressure has a strong influence on increase of nozzle wear (Kovacevic 1990). The variables used in the study the following:

Pressure 207 MPa and 262 MPa.

Abrasive flow rate: 0.453 Kg/min and 0.906 Kg/min.

The following parameters were kept constant:

Diameter of waterjet orifice: 0.33 mm

Diameter of AWJ nozzle: 1.19 mm

Length of abrasive nozzle: 76.2 mm

Abrasive: #80 mesh aluminum oxide.

Traversing speed: 152 mm/min.

Work piece: 6.35 mm thick stainless steel plate.

The wear rate is measured as the change in ID of the nozzle and the general form of the wear process is represented by curves in figure 3.1.

Studies show that typically a tungsten carbide nozzle has an average life time of 4 hours when garnet is used as abrasive, or just 5 min when aluminum oxide is used (Kovacevic 1990). It is clear that the large wear rate in carbide nozzle affect the accuracy and economical operation of the system.

The nozzle wear has to be detected before the nozzle inside diameter exceeds the acceptable limit. Different sensing mechanisms are used for this purpose.

3.3 Disintegration of Abrasive Particles

In AWJ cutting, abrasive particles perform the actual cutting action while the high velocity waterjet accelerate them to the required velocity to enable the cutting. Because of the inefficiency of conventional abrasive entrainment, 70 to 80% of the abrasive particles are fragmented during the mixing and ejection process. Results of experiments show the disintegration process in a typical AWJ system (Simpson 1990).

The setup consisted of an abrasive nozzle assembly utilizing the venturi type abrasive entrainment mechanism, incorporating a sapphire pure waterjet nozzle and a tungsten carbide focussing nozzle.

The following parameters were set for the tests.

Diameter of waterjet nozzle:	0.40 mm
Diameter of carbide nozzle:	1.52 mm
Stand-off distance:	1.50 mm
Type of abrasive:	Silica sand
Abrasive flow rate:	470 grams/min

Sieve analysis was carried out on the standard abrasive to get samples in the ranges of below 150 μm , 150 to 300 μm and 300 to 500 μm . Experiments were conducted at different pressures ranging from 41 MPa to 207 MPa.

3.3.1 Results

The extent of particle disintegration is graphically represented in figure (3.2). It is clear that there is a shift of particle distribution towards a greater percentage of smaller particles. Also it can be noted that percentage of disintegration is more for larger sized particles. The particle disintegration increases linearly with waterjet pressure as shown in figure 3.2.

3.3.2 Factors Influencing the Disintegration

Major factors influencing the disintegration are interaction of particles with carbide tube, interaction between high velocity jet stream and individual particles and the interaction between individual particles.

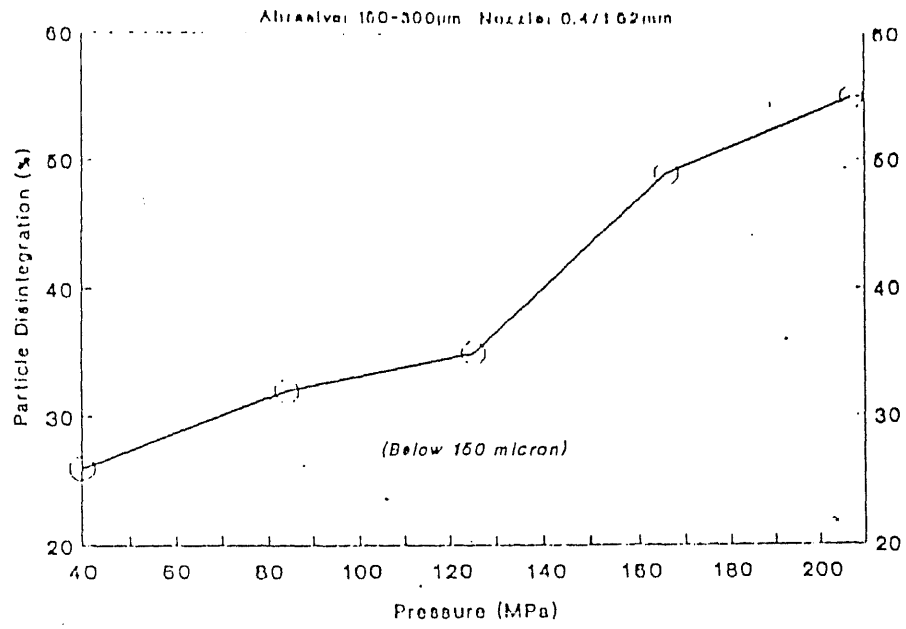


Figure 3.2 Abrasive Disintegration During Ejection

2.3.2.1 Influence of Carbide Tube. Of the several factors influencing the disintegration process, the effect of carbide tube is particularly interesting. The high rate of tube wear indicates that interaction between tube and abrasives is very significant. When the tube diameter increases, particles around the periphery of jet acquire less velocity, resulting in poor cutting performance (Labus 1989). This in turn reduces particle disintegration.

2.3.2.2 Other Factors. The combined effect of interaction between high velocity jet and particles and the interaction between particles themselves was studied experimentally (Simpson 1990). In the experiment, abrasives of size 150 - 300 μm were ejected using a hand held gun into the pure water jet from sapphire nozzle. After retrieving the abrasives from the jet, sieve analysis were performed. About 25% were disintegrated to size below 150 μm , but this time the disintegrated particles were of substantial and uniform size.

This shows that the interaction of carbide tube and abrasive particles is responsible for the fragmentation of abrasives in to fine particles. Disintegration due to interaction of waterjet and particles and due to interaction between particles produce more substantial and discrete particles.

It is clear that there exists potential for the design of a new AWJ nozzle by eliminating the carbide tube and there by reducing particle disintegration nozzle wear.

CHAPTER 4

THE PROPOSED DESIGN

4.1 General principle

The new design is aimed at eliminating the problems in the conventional abrasive entrainment mechanism. The design is based on “Annular Jet Principle”, invented by Harnoy, which was presented to the patent committee of NJIT in May, 1990. The abrasive entrainment system is modified for a new flow pattern as shown in figure 4.1. The high velocity waterjet and abrasives are mixed outside the nozzle. Abrasive particles mixed with low pressure water form a jet which is merged with the high velocity pure waterjet. In the new design (figure 4.1), high pressure water is supplied from port 1 and form a high velocity jet. Low pressure water and abrasives are pre-mixed and supplied through port 2 to the annular space. Since port 2 is off the vertical axis, the mixture swirls inside the annular space. Subsequently, the mixture pass through the annular clearance between the inner conical cylinder and the surrounding annular sleeve. This forms a low velocity jet surrounding the central high velocity jet and they merge outside the nozzle.

4.2 Design Procedure

The design and development of the new nozzle was carried out in two stages. Stage 1 involved development of prototype nozzle to test the principle. Upon verification of the principle, a fully operational prototype was developed in stage 2. Subsequently, experiments were conducted to evaluate the performance.

4.3 Stage 1: Design for Low Pressure

It was decided that before proceeding to the design of an operational model, a preliminary model nozzle has to be developed to verify the principle. The nozzle was designed to test using low pressure supply water.

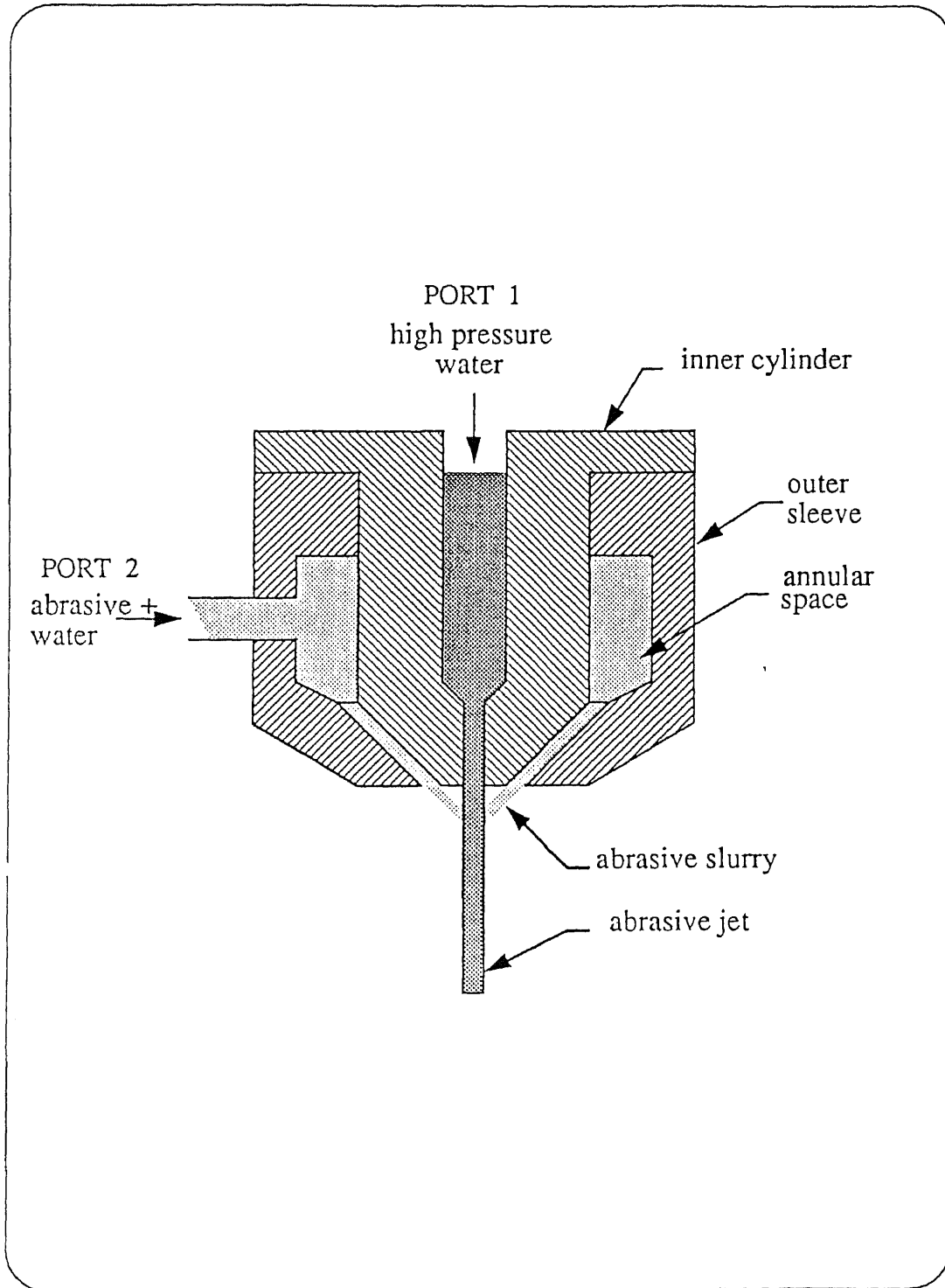


Figure 4.1 Preliminary Design for Low Pressure.

4.3.1 Nozzle

The nozzle is an assembly of two parts as shown in figure 4.1. Two inlet ports are provided for connecting the main supply and the abrasive mixture. Main supply is connected to port #1 which flows axially downwards to form the main jet. Abrasive particles and water are pre-mixed at the mixing tube and the mixture enter through port #2 into the annular space between the inner cylinder and outer sleeve. The inlet at port #2 is off the center line of the nozzle which creates swirling of abrasive mixture inside the annular space. Since the abrasive particles are denser than water, they tend to settle down at the bottom. The swirl of the abrasive mixture helps to keep the particles suspended in water. The mixture flows down through the annular slit between the two parts and generate a thin jet surrounding the central jet. The two streams merge outside to form a single jet.

4.3.2 Mixing Tube

Abrasive particles and water are pre-mixed outside before feeding into the nozzle. A mixing tube as shown in figure 4.2 is used for this purpose. The arrangement is similar to a 'tee' connection of pipe. One end of the horizontal section is connected to supply water through 1/4" plastic tube. The converging zone at the inlet helps to accelerate water through the horizontal section. Abrasive powder is fed through the vertical inlet into the stream. A straight 3/8" transparent plastic tube is connected to the vertical inlet. The mixture of water and abrasive exit through the opposite end of the horizontal section. A valve is attached to the inlet tube to regulate the flow of water. When the valve is turned on, water rise along the vertical tube and gets balanced at a height. The abrasives fed through the top of the vertical tube reach the water column and proceed downwards along the tube to mix with the horizontal stream of water. The outlet section of the mixing tube is welded to the abrasive inlet port of the nozzle.

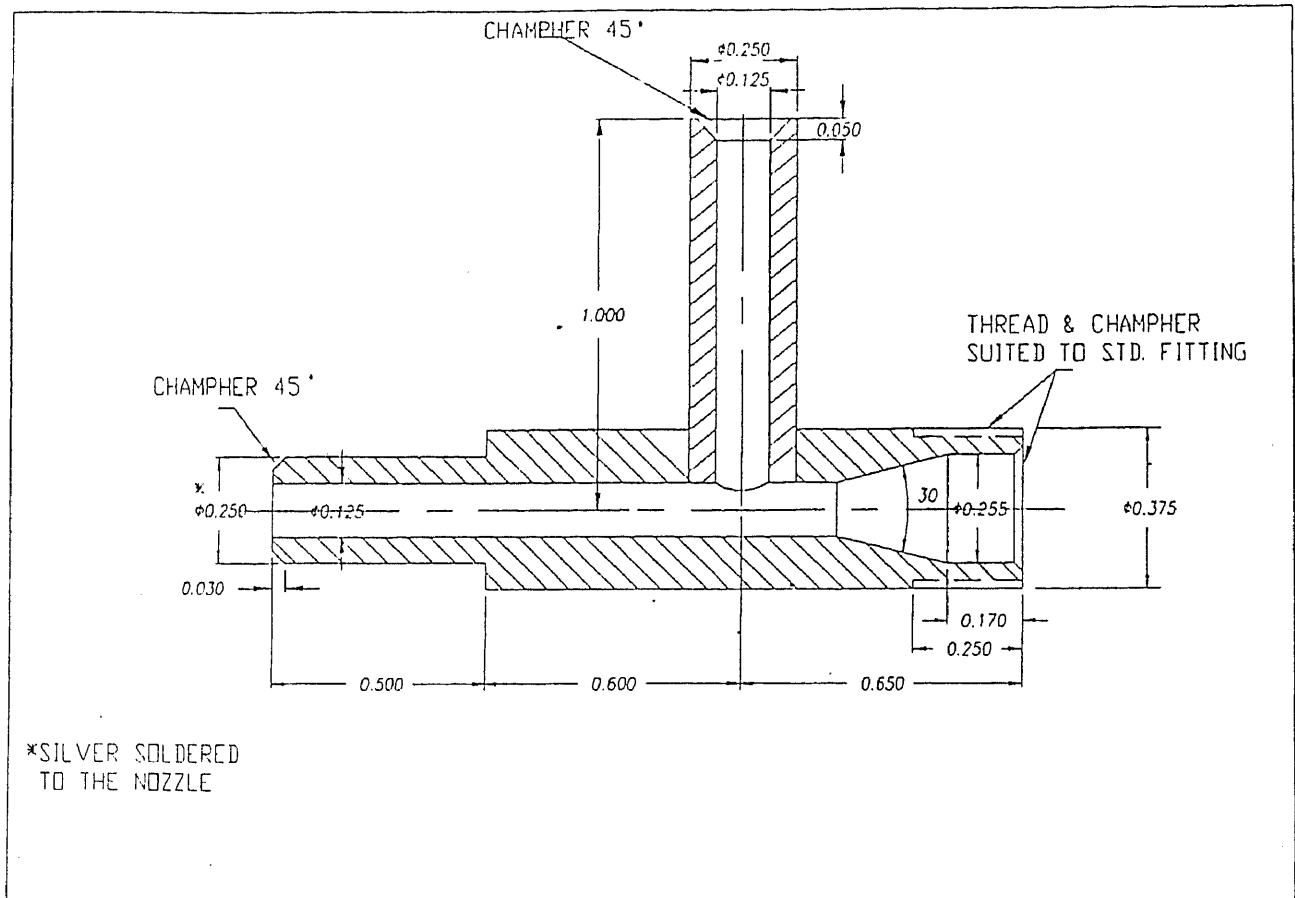


Figure 4.2 Mixing Tube.

4.3.3 Adjustment of Abrasive Flow

Arrangement has been provided for varying the flow rate of abrasive mixture in the nozzle. By turning the screws on top of the nozzle, the inner part can be moved up or down. This changes the clearance of the annular slit between the two parts. To increase the flow rate, the clearance is increased and vice versa.

4.3.4 Experiment Setup

The experiment setup is shown in figure 3.4. The nozzle assembly is mounted on a supporting bracket attached to a tank. Supply water is connected to inlet port 1 using a flexible 1/4" plastic tube. Valve 1 regulates the flow rate. A similar connection is made to the inlet of mixing tube through valve 2. For abrasive feed, a vertical connection is made to the mixing tube. The water from the nozzle is collected in the tank.

4.3.5 Operation

Using the adjustable screws on top of the nozzle, the clearance of the annular slit inside the nozzle is adjusted to about 0.5 mm. Valve 1 is turned on so that the main jet is formed. Next, valve 2 is gradually turned on. Water starts to rise along the vertical inlet of the mixing tube. By adjusting valve 2, the water column in the vertical tube is balanced at a height of approximately 8 inches. Since the inlet from the mixing tube is off the vertical axis of the nozzle, water swirls inside the annular space of the nozzle. Some of this swirling action is carried over to the secondary jet also. Due to this, the secondary jet has a tendency to diverge. Experiments show that the spacing of the annular slit is critical to form a jet. When the clearance of the slit is less, the friction of the walls is sufficient to dampen this circulation.

Once the flow is stabilized, abrasives are fed manually through the top of the vertical section on mixing tube. The abrasive used for the experiment is of size #120. Abrasive feeding is carefully controlled to make sure that the feed is uniform. Although

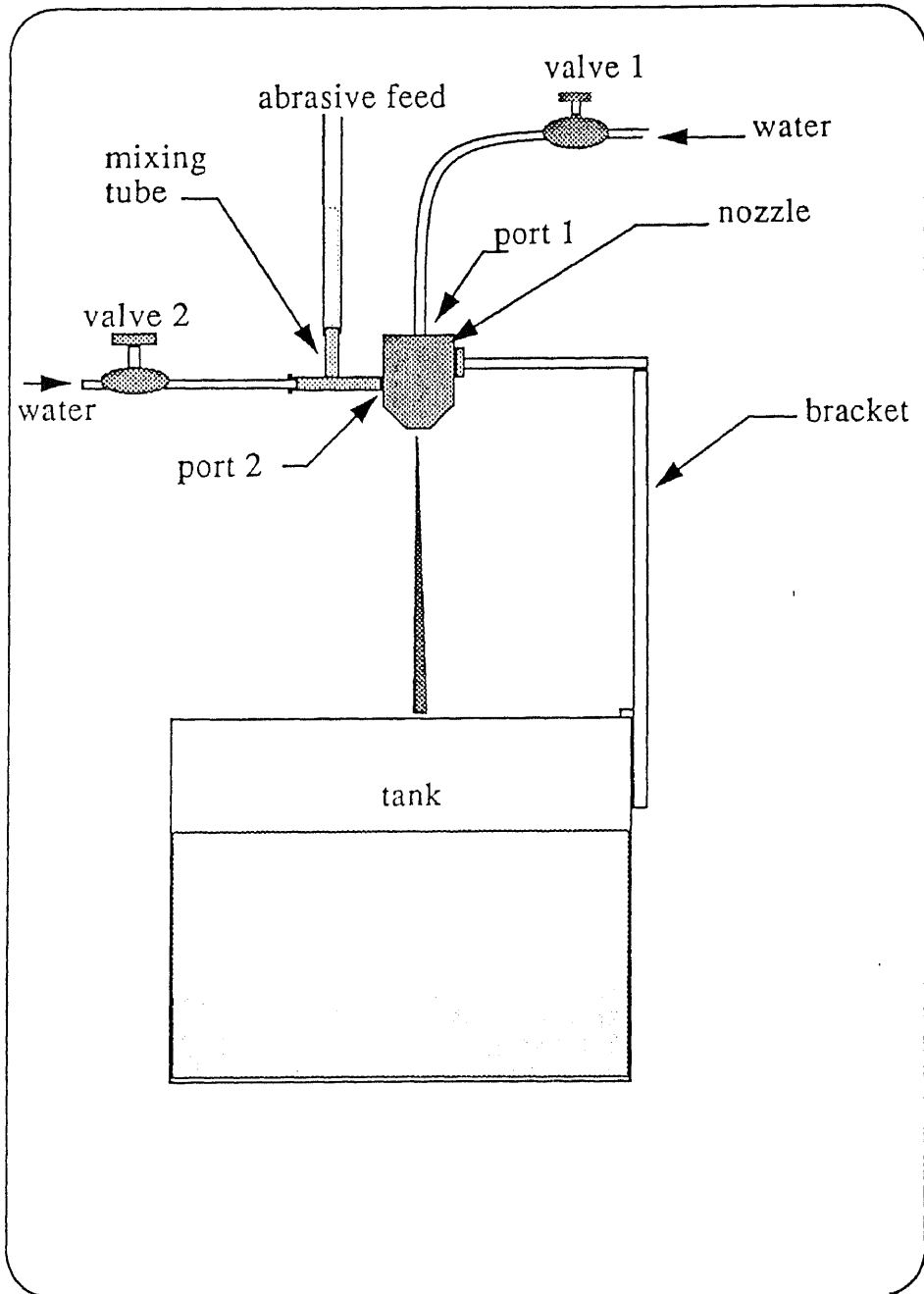


Figure 4.3 Experiment Setup for Preliminary Model.

small clearance of the slit is suitable for the proper formation and merging of the secondary jet, it inhibits the abrasive flow. This may result in clogging of abrasives inside the nozzle. Thus a trade off is necessary for the proper formation of the jet as well as proper flow of abrasives.

The experiments showed that by carefully adjusting the clearance of the annular slit and regulating the water flow rate and abrasive feeding, proper mixing of the two jets can be achieved.

4.4 Stage 2: Design and Development for high Pressure

Upon verification of the operating principle, design of the prototype nozzle for high velocity was carried out. The general configuration is essentially the same as the previous one, but adequate strength has to be ensured for operating under pressure as high as 50,000 psi and jet velocity of up to 800 m/sec. Since sapphire nozzle is used in the existing AWJ systems for producing the thin, high velocity water jet, it was decided to incorporate sapphire in the new design. Another main consideration was to ensure that the replacement of the existing nozzle with the new one would not require any modification to the set up of the water jet cutting machine. The detailed drawing of the modified nozzle is given in appendix A.

The material used for making the nozzle is alloy steel. The nozzle assembly is shown in figure 4.4. A solid model of the nozzle is shown in figure 4.5. The inner cylinder (part# 2) is modified to accommodate the sapphire. Through the inlet at the top, sapphire is inserted which glide through the hole and rest on the curved seating provided. High pressure water from intensifier is connected to the top of the inner part. Suitable threading is provided match with the high pressure outlet of the water jet cutting machine. To eliminate any potential leakage of water, an insert is provided which directly connect the inlet and the top of the sapphire. The outer sleeve (part# 1) provides the annular space when mated with the inner part. Inlet for the abrasive - water

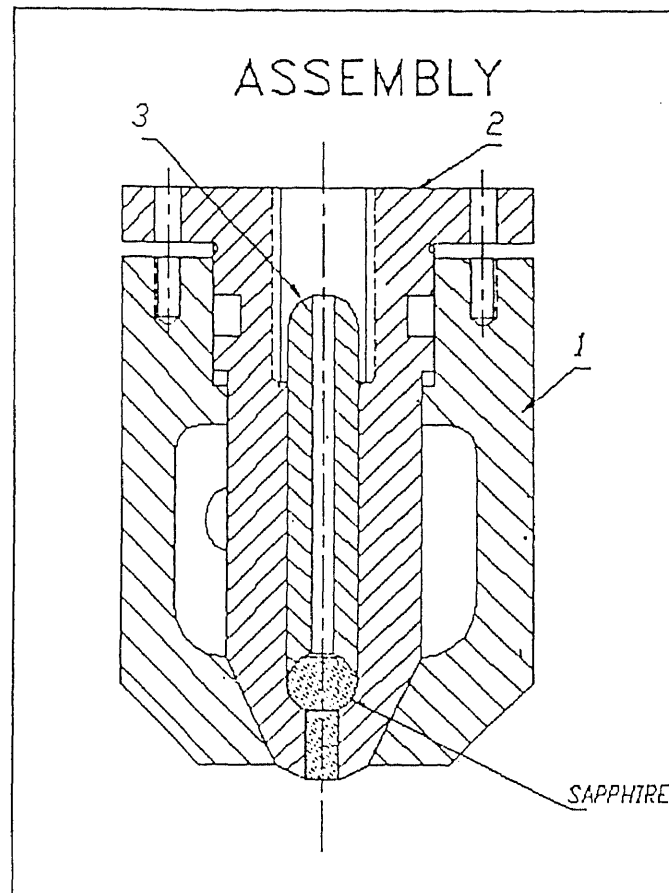


Figure 4.4 Nozzle Assembly for High Pressure.

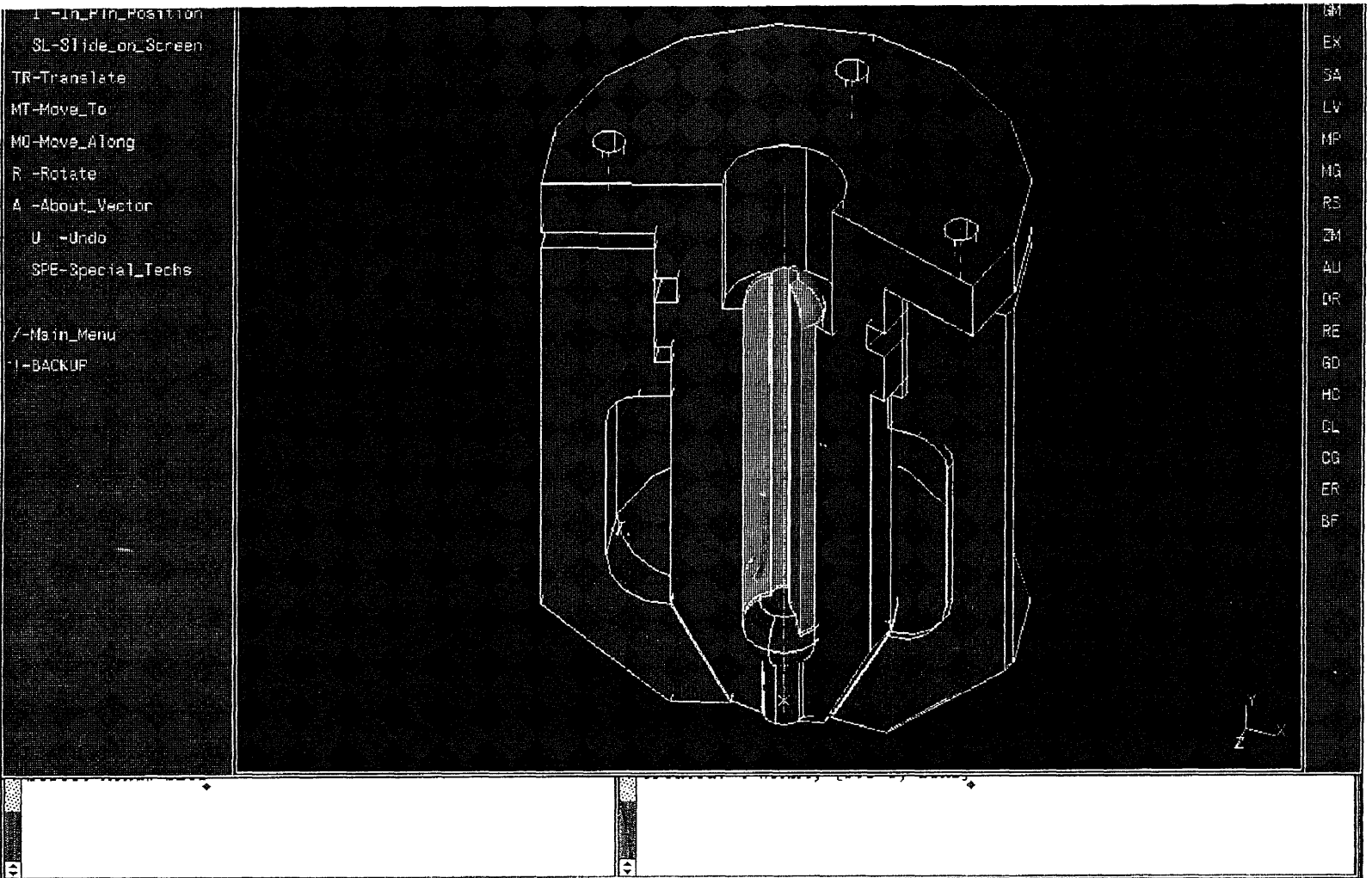


Figure 4.5 Solid Model of the Nozzle Assembly.

mixture is from the side through the hole which is off the central axis of the nozzle. The inner part can be moved up and down by turning the screws on top of the nozzle. By doing so, the clearance of the annular slit can be adjusted. An 'O' ring is provided to prevent leakage of abrasive mixture through the top.

4.4.1 Strength Calculation for the Inner Cylinder

The bottom of the inner part is the critical region which has to with stand the high pressure. The seating of the sapphire is contoured to reduce stress concentration. Figure 4.6 shows the arrangement.

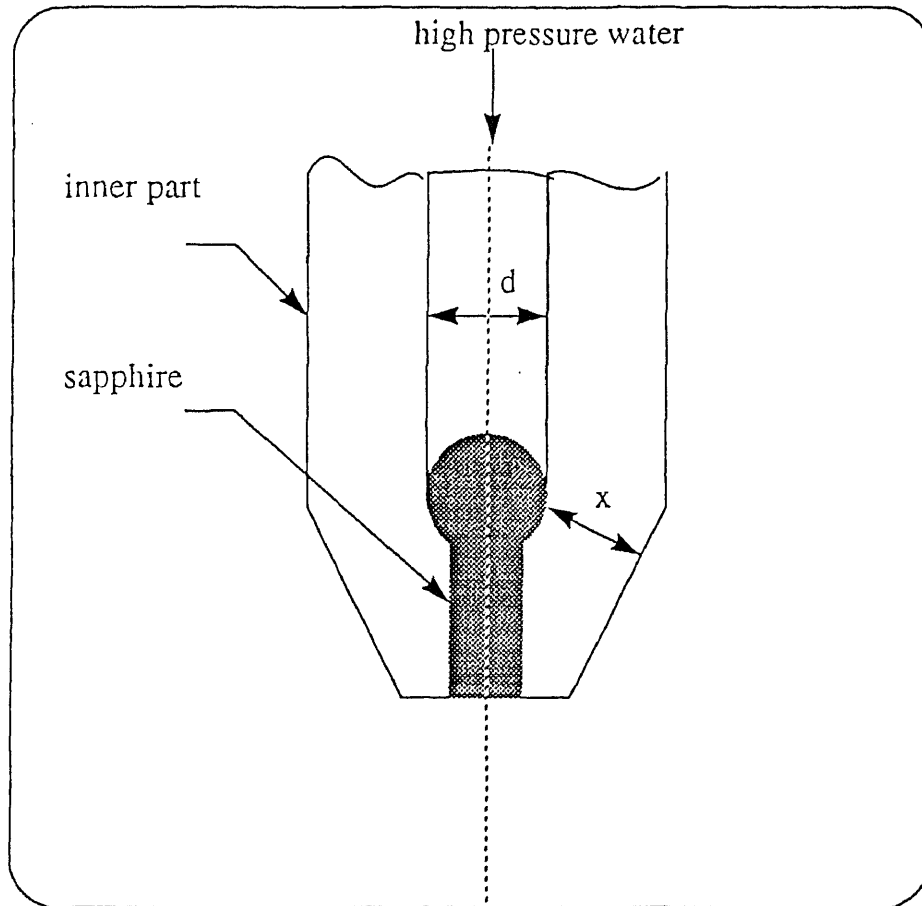


Figure 4.6 Critical Region of Inner Cylinder.

operating pressure $p = 50,000$ psi.

diameter of sapphire $d = 0.25$ "

$$\begin{aligned} \text{area } a &= pd^2/4 \\ &= p \cdot 0.25^2/4 \\ &= 0.05 \text{ in}^2 \end{aligned}$$

$$\begin{aligned} \text{load } F &= p / a \\ &= 50,000 \text{ (lb/in}^2\text{)} / 0.05 \text{ in}^2 \\ &= \underline{2500 \text{ lb.}} \end{aligned}$$

load bearing area

wall thickness $x = 0.15$ in.

$$\begin{aligned} \text{load bearing area } A &= p[(d + 2x)^2 - d^2]/4 \\ &= p[0.65^2 - 0.25^2]/4 \\ &= 0.28 \text{ in}^2 \end{aligned}$$

$$\begin{aligned} \text{tensile stress } s &= F/ A \\ &= 2500 \text{ lb} / 0.28 \text{ in}^2 \\ &= \underline{8929 \text{ lb/ in}^2} \end{aligned}$$

yield stress of alloy steel $s_t = 42,000$ lb/in²

$$\begin{aligned} \text{factor of safety} &= s/s_t \\ &= 42,000 \text{ (lb/ in}^2\text{)} / 8929 \text{ (lb/ in}^2\text{)} \\ &= \underline{4.7} \end{aligned}$$

4.4.2 Experiment Setup

Some experiments were performed using the new nozzle to evaluate the performance. At this stage, the experiments are not complete and hence the cutting performance of the nozzle is not fully analyzed.

Ingersoll-Rand CNC waterjet cutting machine was used for the experiments. Since the nozzle is compatible to the existing connection of the waterjet cutting

machine, the change over can be done easily. The pressure of the intensifier was set to 40,000 psi and supply water at 60 psi was connected to the abrasive mixing tube. The vertical inlet of the mixing tube was connected to the existing abrasive feed mechanism which supplied #120 size abrasives. The sapphire used in the nozzle was of size 0.014".

4.4.3 Abrasive Feed

The abrasives feed is through a vibrating chute and the feed rate can be continuously varied by changing the vibration amplitude of the chute. This mechanism provide accurate control of the abrasive feed. The chute is connected to the vertical inlet of the mixing tube via a 3/8" flexible plastic tube. The abrasive particles falling from the chute reach the mixing tube by gravity. The supply water causes the water to rise along the vertical tube to balance the pressure. Abrasives from the feeder reach the surface of the water column and then move down along the water column to reach the mixing tube. Since the inner wall of the abrasive feeding tube was wet, abrasives tend to stick to the wall and this could result in clogging inside the tube.

4.4.4 Operation

The objective of the experiment was to make 3" long cut on a work piece of 2 mm thick aluminum sheet. Abrasive feed rate, water flow rate for the abrasives, stand off distance and the speed of cut were varied to study they affect the cutting. The effects of varying these parameters is analyzed.

4.4.5 Results

Several cuts performed by varying the parameters are compared with a cut using pure waterjet. Pure water jet made a cut of about 1 mm. depth and 1.5 mm width with sharp and smooth edges.

4.4.5.1 Effect of Abrasives The cuts made with abrasives were slightly deeper than that of pure waterjet, but not sufficient to make the complete cut. Also, along the sides of the cut, scattered marks were found as a result of the scattered abrasives on the periphery of the jet. As the feed rate increased, the depth of cut improved but since this resulted in clogging of abrasives inside the nozzle. For this reason, the abrasive feed rate was limited.

4.4.5.2 Effect of Flow Rate of Supply Water for Abrasives Since supply water was used as a carrier for abrasives, the flow rate had to be sufficient to transport the relatively heavier abrasive particles. Since Abrasive feed and water flow rate were inter dependent, water flow had to be increased to increase abrasive feed. But increasing the flow rate had a tendency to diverge the jet, resulting in poor cut.

4.4.5.3 Effect Stand off Distance In the new design, abrasives and high velocity jet are mixed outside the nozzle. The jet imparts momentum to the abrasive stream and the particles get accelerated. For the abrasives to acquire sufficient velocity, the mixture has to travel certain distance from the mixing position.

In the experiment, stand off distance was varied from 5 mm to 30 mm. The increase of stand off distance resulted in increased scattering of abrasives. This reduced the cutting performance. The reason for scattering is believed to be the higher flow rate of supply water.

4.4.5.4 Effect of Speed of Cut: The cutting speed was varied from 25 mm/min. to 100 mm/min. Reducing the speed resulted in better cutting.

4.4.6 Conclusions

The general principle of the proposed design is valid, but more extensive experiments

are to be done to evaluate this. The experiments showed that by increasing the abrasive feed rate, the cutting can be improved. But due to the limitation of the mixing tube arrangement, the feed rate was limited. The possible way to increase the feed was to increase supply water flow, but this increased the divergence of the jet. It is expected that the cutting can be improved by using more abrasives and less supply water. Further work has to be done to this end to increase the abrasive content in the abrasive-water mixture.

CHAPTER 5

FLOW SIMULATION

5.1 General

Traditionally, the approach to engineering design has been to construct a physical model and perform experiments to gather the “data” affecting the design decision. The recent advancement of computer technology and computational mechanics has simplified the task of gathering the “data” by the use of numerical models which can simulate the experiments.

Numerical simulation has several advantages. The computational approach can save substantial amount of time and expenses involved in physical experiments. Various conditions, some of which are even unattainable in laboratory set up, can be modeled using numerical methods. Another advantage is that disturbances and inaccuracies associated with the lab equipment eliminated in numerical simulation. Though numerical simulation cannot fully substitute laboratory experiments, it can eliminate some of the preliminary tests and the designer can come up with an improved prototype for the experiments.

5.2 FIDAP fluid dynamics analysis package

FIDAP is a general purpose computer program for the analysis of incompressible fluid flows. Finite Element Method (FEM), which is widely used for structural and thermal analysis, is the solution method used in FIDAP. In FEM, the domain of analysis is divided in to small elements. The partial differential equations for the flow domain are replaced by a set of ordinary differential and algebraic equations for each element. By using numerical methods, these equations are solved simultaneously to obtain the various parameters like velocities, pressures and temperatures.

5.3 FIDAP structure

FIDAP package consists of several programs which are grouped in to three modules and each executed in different stages of the operation. The 3 stages of operation are pre processing, processing and post processing.

5.3.1 Pre- processor (FIPREP Module)

The first stage of the execution is called pre processing. The function of pre processor is to gather all the input data required for the problem and format the data for subsequent presentation to the processing module. The control program of pre processor is called FIPREP. In pre processing, the geometry of the flow domain is defined and finite element mesh is generated via the program FIMESH. Physical properties of the fluid, boundary conditions and initial conditions are specified. The information about the type of solution procedures is also input in this stage.

5.3.2 Processor (FIDAP Module)

This is the stage where computations are performed. The input data for this module is presented by the pre processor. The governing partial differential equations are transformed in to algebraic equations and solved using iteration procedure. This stage is the 'number crunching' stage involving extensive computations.

5.3.3 Post- processor (FIPOST Module)

In this stage the out put of the processing stage is formatted and presented to the user. The results of the analysis are displayed graphically for better visualization.

All model definition data is prepared using FIPREP and the analysis of the results is performed using FIPOST. There is no user interface with the processing module FIDAP.

5.4 Modeling of Turbulence

The flow of the high velocity jet is essentially turbulent and hence a suitable model is chosen for the analysis. Generally the flows of practical and industrial relevance are almost always turbulent, which means that the flow is highly random, unsteady and three dimensional. Due to this, the task of modeling turbulent flow is complex. In order to describe turbulent flows completely, time dependent three dimensional governing equations are to be solved. Since turbulent motion contains scales which are much smaller than the extent of the flow domain, the solution of the time dependent governing equations demand extremely fast and large scale computing that are not available today. For this reason, the turbulent motion is described in terms of time averaged quantities rather than instantaneous ones.

Two possible models are available for modeling turbulence - Prandtl's mixing length model and the k - ε model. Both are based on Reynolds averaged equations and use the eddy viscosity concept. In these models, time averaged Navier Stokes and energy equations are solved.

5.4.1 Mixing Length Model

In this model, the effective viscosity μ_e is computed as:

$$\mu_e = \mu_o + \mu_t$$

where μ_o is the laminar viscosity of the fluid and μ_t is the turbulent viscosity. The turbulent viscosity is computed using Prandtl's mixing length approach. i.e.,

$$\mu_t = \rho l m^2 \left| \frac{\partial U}{\partial y} \right|$$

where the unknown parameter $l m$ is the mixing length, whose distribution over the flow field has to be prescribed using empirical information, ρ is the density and dU/dy is the velocity gradient.

5.4.2 k - ε model

This is more sophisticated model where the turbulence field is characterized in terms of two variables - the turbulent kinetic energy k and viscous dissipation rate of kinetic energy ϵ .

The effective viscosity μ_e is computed as:

$$\mu_e = \mu_o + \mu_t$$

Turbulent viscosity μ_t is computed by solving two additional transport equations - one for turbulent kinetic energy k and another for turbulent dissipation ϵ .

$$\mu_t = \rho c_\mu \left(\frac{k^2}{\epsilon} \right)$$

where c_μ is an empirical constant.

k and ϵ are calculated using the following equations:

$$k = I U^2 / 100$$

$$\epsilon = k^{1.5} / L$$

where I is the turbulence intensity level expressed as a percentage, U the velocity magnitude and L the characteristic eddy length.

5.5 Solution Procedure

5.5.1 Problem Definition

In the proposed design, high velocity waterjet and abrasive stream are mixed outside the nozzle to form the abrasive jet. The primary objective of the simulation is to study the mixing of the two jets. Hence the flow domain chosen for the analysis is as shown in figure 5.1 . High velocity waterjet emanates from the sapphire which is mounted at the bottom of the nozzle. The abrasive stream emanating through the annular slit merges with the central jet and gets accelerated. The flow domain include the region inside the sapphire, annular slit, mixing region and the acceleration region. Since the

FIDAP package does not have the capability of modeling fluid-solid mixture, true modeling of the abrasive stream is not possible. For this reason, abrasive - water stream is simply considered as pure water stream.

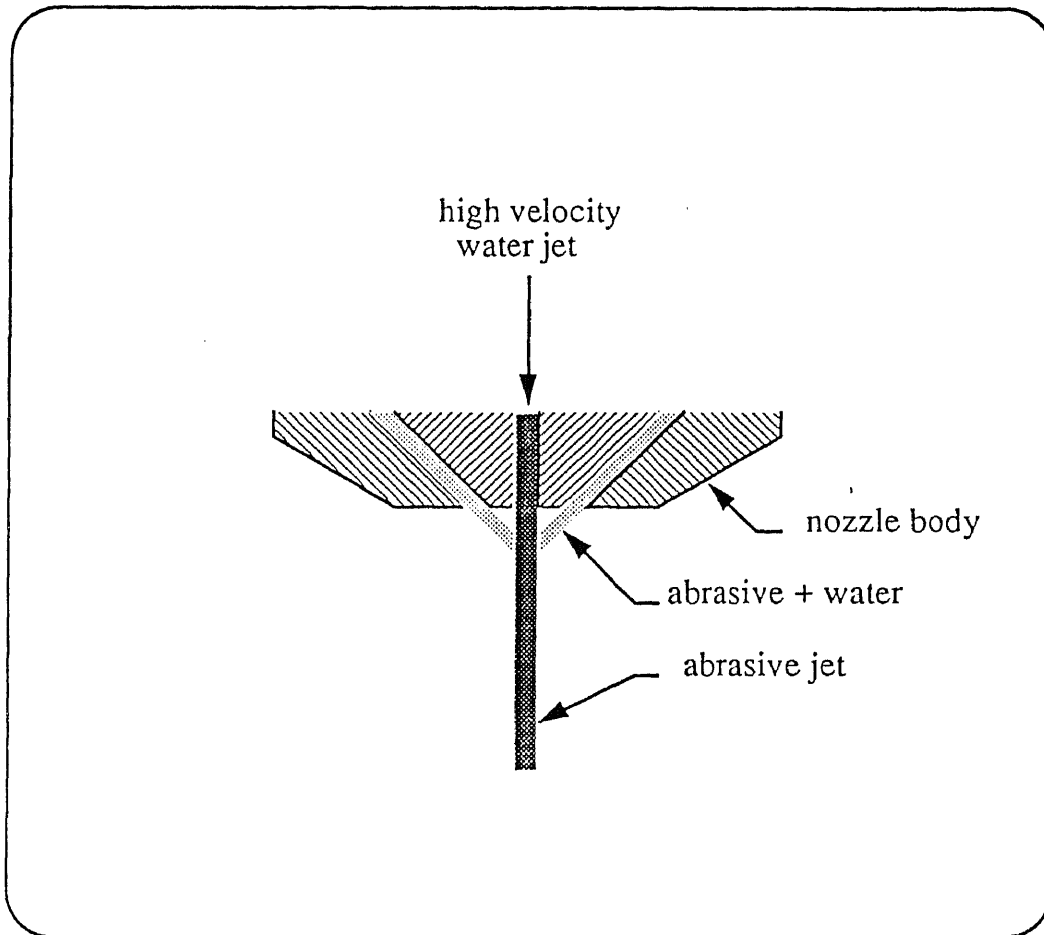


Figure 5.1 Flow Domain.

5.5.2 Definition of Geometry

The solution procedure begins with the defining the geometry for the region of analysis. Figure 5.2 illustrates the geometry. As the solution of turbulent model involve substantially long computing, every attempt has been made to simplify the geometry.

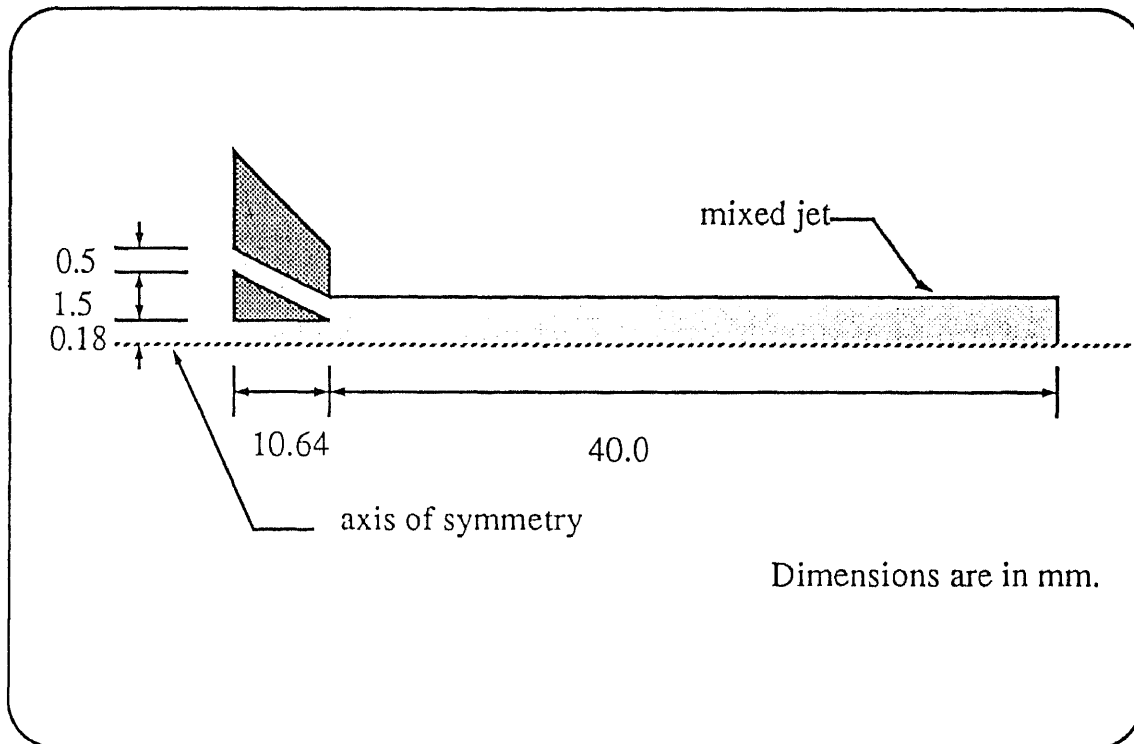


Figure 5.2 Definition of Geometry.

Since the flow is axi-symmetrical, only one side of the axis of symmetry has to be defined for the analysis. The diameter of the sapphire is 0.014"(0.36 mm). Hence the radius of the high velocity jet at the inlet is $0.36/2 = 0.18$ mm. The length is 10.64 mm. The clearance of the annular slit is taken as 0.5 mm. A 40 milli-meters long region of the mixed jet is considered to be sufficient to study the mixing characteristics.

5.5.3 Non-dimensionalization of Geometry

The analysis can be performed in either dimensional form or non-dimensional form. In the case of dimensional input, the geometry and all other parameters like velocity, viscosity, kinetic energy etc. are to be input with dimensions. FIDAP has the capability of handling SI and English units. In this case the output of the calculations will be with dimensions.

The non-dimensional input is another simple way of specifying the geometry and other parameters. In this method, a reference dimension is chosen and all other dimensions are specified as multiple of this dimension. In this model the inlet diameter of the sapphire (0.18 mm) is taken as the reference.

5.6 Boundary Conditions

Rotational symmetry is assumed so that axi-symmetric analysis can be performed. The axial direction is referred as Z direction and the radial direction is called R direction. The flow is two dimensional, steady and both laminar viscosity and density are assumed to be constant. Tangential components of velocity are assumed to be zero. The walls are smooth and impermeable. Figure 5.3 illustrates the boundary conditions.

5.6.1 Velocity

5.6.1.1 Inlet. The inlet velocity of the high pressure jet is taken as 700 m/s. This is changed to non-dimensional form and given as 1 unit. This is taken as the reference

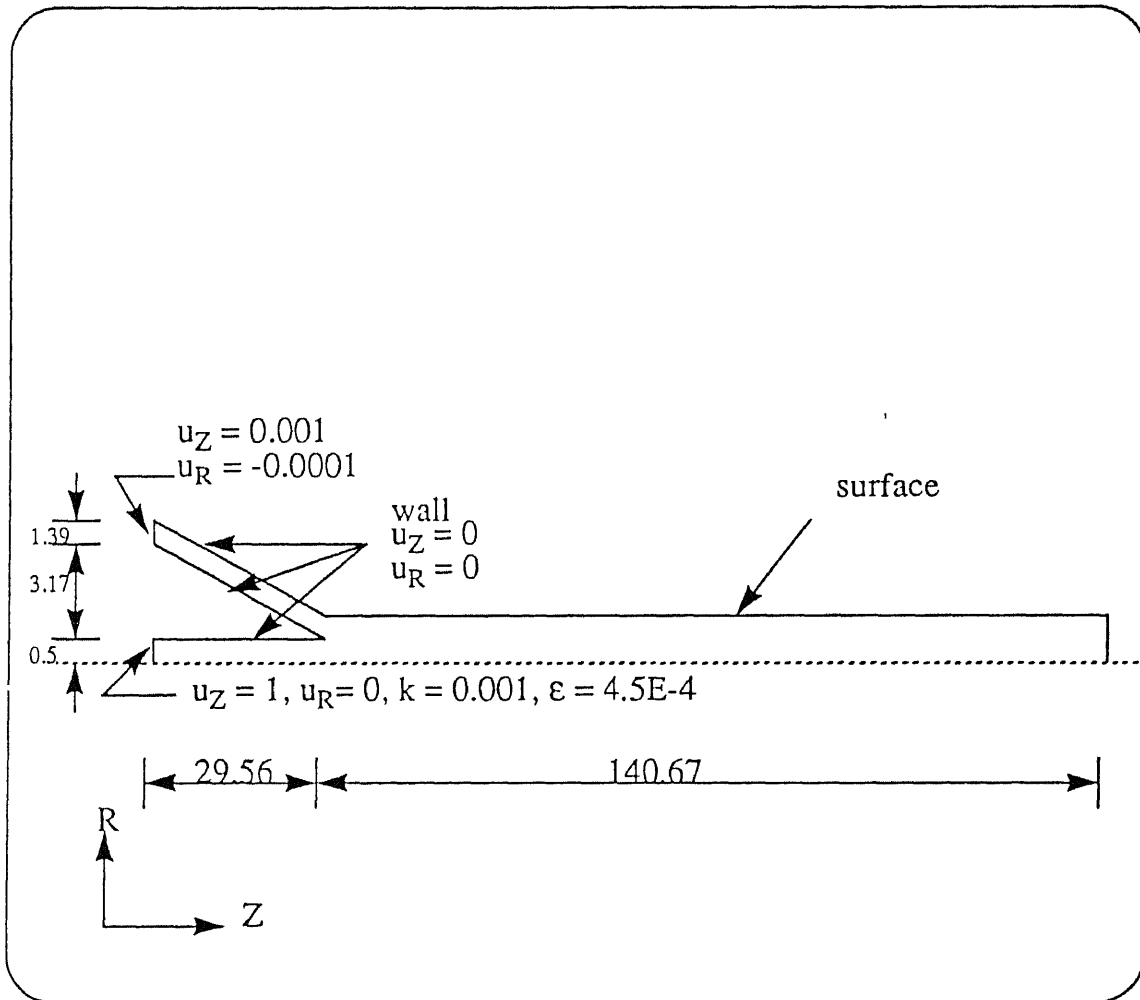


Figure 5.3 Boundary Conditions.

velocity. Radial component u_R is zero. For the abrasive flow is at an angle to the axis of the nozzle. Hence it has both axial and radial components which are input as a fraction of the reference velocity. i.e. $u_Z = 0.001$, $u_R = 0.0001$.

5.6.1.2 Walls. The wall surfaces inside the nozzle are considered smooth, rigid and impermeable. It is assumed that no slip boundary condition is valid for walls. Hence velocity components assume zero velocity at wall.

As the k - ϵ turbulence model is not valid in the viscosity affected regions close to the wall, an approach called 'near wall modeling' is used in the close proximity of the solid walls.

5.6.2 Turbulent Kinetic energy k

Kinetic energy k is specified at the inlet position. k is calculated using the expression:

$$k = I.U/ 100$$

where I is the intensity level expressed as a percentage and is assumed as 10. U is the absolute magnitude of the velocity vector and equal to 1.0.

5.6.3 Turbulent Dissipation ϵ

Turbulent dissipation ϵ is specified at the inlet region. ϵ is calculated as:

$$\epsilon = k^{1.5}/ L$$

where L is an empirical parameter called characteristic eddy length for turbulent flow and is taken as 0.07.

$$\begin{aligned} \epsilon &= 0.001^{1.5}/ 0.07 \\ &= \underline{4.518 \times 10^{-4}} \end{aligned}$$

5.6.4 Viscosity

The viscosity is expressed in terms of a dimensionless parameter, the Reynolds number

and is defined as:

$$Re = \rho UL/\mu = Ud/\nu$$

$$\text{where } \nu = \mu/\rho$$

ν is the kinematic viscosity = 1.3099 mm²/sea for water at 50° F

U = velocity at inlet = 7×10^5 mm/sea

d = diameter of sapphire inlet

$$= 0.36 \text{ mm.}$$

$$Re = 7 \times 10^5 \cdot 0.36 / 1.3099$$

$$= 1.924 \times 10^{-7}$$

Reference viscosity = $1/Re$

$$= 1/1.924 \times 10^{-7}$$

$$= \underline{5.198 \times 10^{-6}}$$

5.7 Initial Conditions

The initial values for the various parameters such as velocity and temperature are input for the solution. For a transient analysis, the parameters of solution varies with time. Hence, the values input here are used as the initial condition at the initial time. For a steady state analysis, the initial conditions serve as an initial guess for the non-linear iterative solution method. Certain problems such as free surface problems can only be solved in stages. In these cases the solution of the first stage is taken as the initial guess for the second stage and so on. This method is described in the following section where free surface problem is described in detail.

In the current problem, values of turbulent kinetic energy k and turbulent dissipation ϵ are input as initial conditions. The values of these parameters given in the boundary are initially set for the whole region.

5.8 Free Surface Boundary

The jet emerging from the nozzle is free and hence the boundary is defined as free surface. The modeling of free surface is more complex compared to fixed boundaries because the nodes on the boundary have additional degrees of freedom. A free surface may be a physically moving boundary, an interface between two fluids or simply the free moving surface of the fluid.

5.8.1 Two stage Approach for Solution

Problems involving free surfaces are solved in two stages. The convergence of free surface problems is very slow, especially if turbulence is involved. Since both free surface and turbulence are involved in the current problem, the two stage approach is employed for the solution. This procedure gives a better convergence.

5.8.1.1 Stage 1. Even though the position of the free surface is unconstrained, initially the boundary is assumed to be fixed with 'slip' capability. In this first stage, axial and radial components of velocity are input as zero. By solving this model, an approximate solution is obtained.

5.8.1.2 Stage 2. In the second stage, the constraints imposed on the boundary are released, and the problem is solved using the out put of first stage as the initial conditions. The initial finite element mesh is automatically modified in this stage to accommodate the deformed boundary due to free surface effect.

5.9 Mesh Generation

In finite element method, the accuracy and cost-effectiveness of the solution is to a large extent dependent on the finite element mesh discretization employed. The mesh can be generated by hand, but this is a tedious and error prone task. Most of the finite

element packages have the capability of auto mesh generation and is highly desirable for three-dimensional problems.

The general strategy for mesh generation is to distribute the nodal points according to the anticipated field variables. For large gradients in the field variables, the mesh should be dense; and for small gradients, the mesh should be sparse.

The mesh generation is done by trial and error procedure. The mesh generated can be graphically displayed and visually checked. Once a satisfactory mesh is generated, the model is solved to get the approximate solution. Upon analyzing the results, the mesh can be refined to distribute the mesh density according to the gradients of the field variables.

The initial mesh generated based on the fixed boundary is shown in figure 5.4. The surface is parallel to the axis of the jet. In the second stage, boundary of the jet is treated as free surface. The deformed mesh generated after the solution is shown in figure 5.5. The divergence of the jet is clearly evident.

5.10 Solution

The first stage of the solution is pre-processing. FIPREP is the module which handle the user input for the problem. The complete information about the problem is input either interactively or in batch mode. In batch mode execution, the data is input as a file named FIINP. Any errors present in the file is reported during the processing stage. These errors are corrected and the file is input for processing. The input file for the first stage is listed in appendix B. Input file for the modified surface boundary is given in appendix C.

The pre-processor generates mesh data and present all input data to the processor called FIDAP. The processor can be run only in batch mode, using the input file FDINP from the pre-processor. This stage is computation intensive and takes about 80% of the execution time.

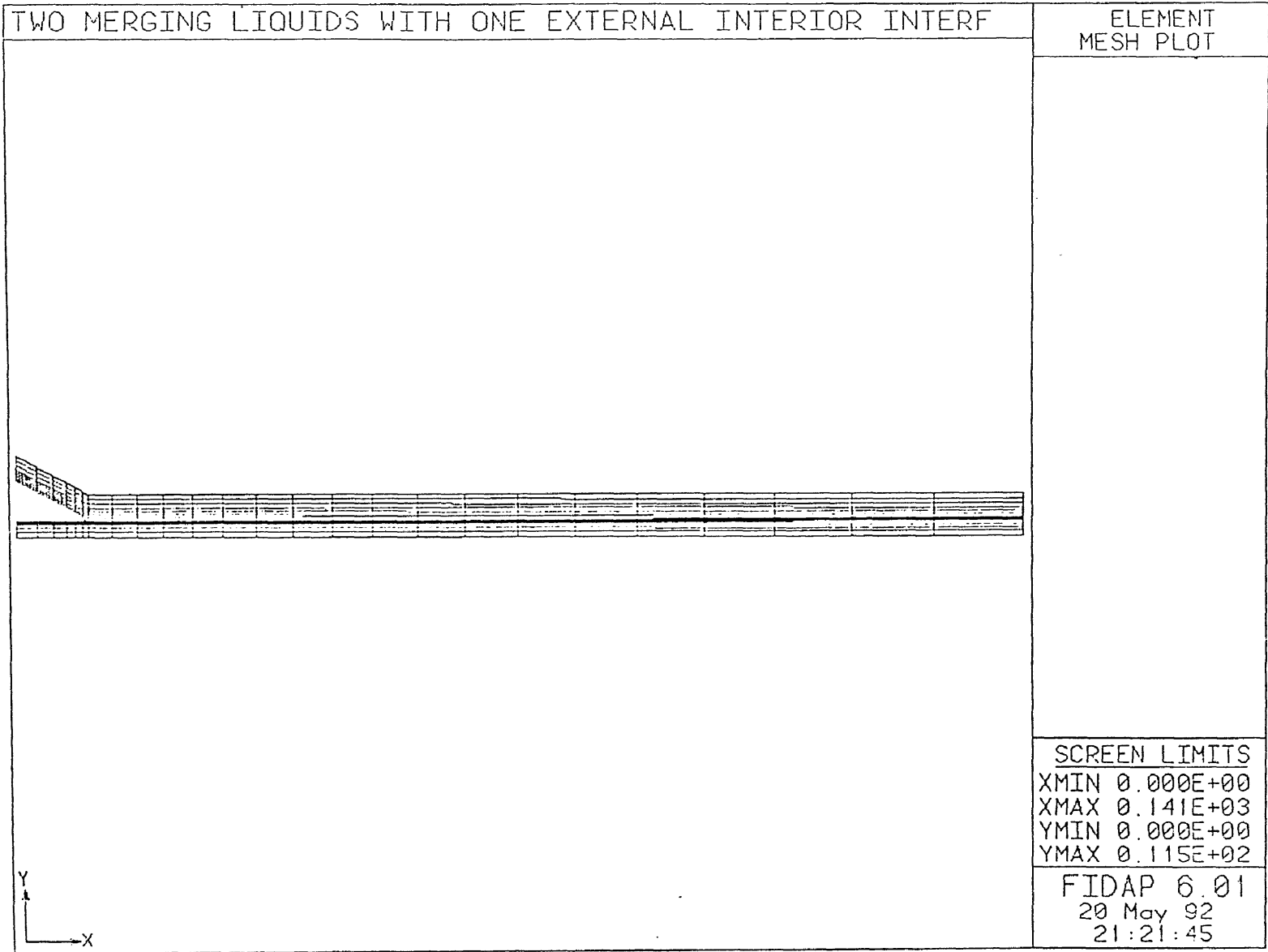


Figure 5.4 Initial Mesh for Trial Solution.

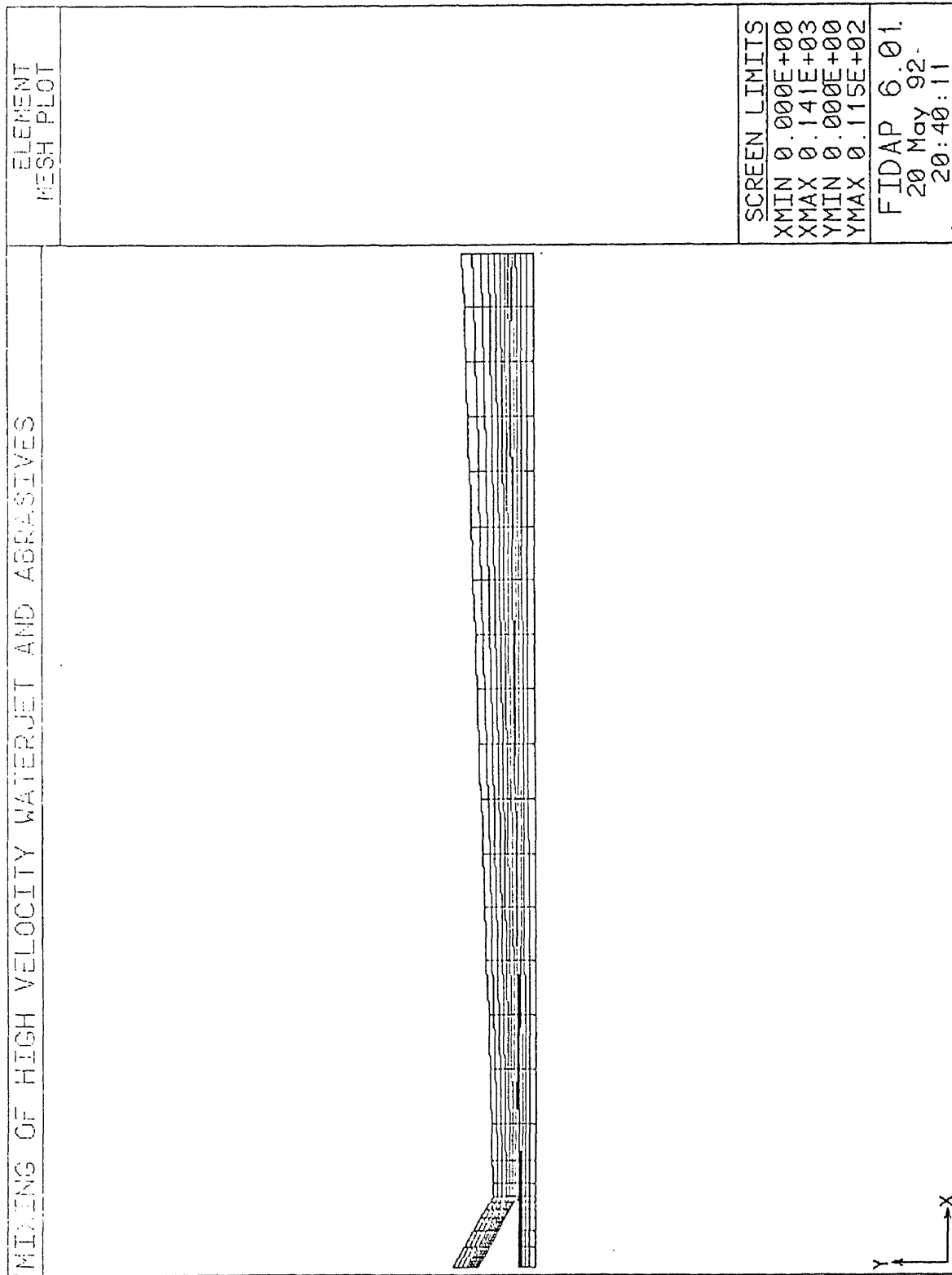


Figure 5.5 Deformed Mesh After Final Solution.

The results of the processor are output in a file named FDPOST. This is used as the input for the post-processor FIPOST where the solution is displayed graphically. Post processor runs in interactive mode.

5.10.1 Solution Methods

The solution procedure employed in the processor is iterative, and several iterative methods are available. The methods available are Successive substitution (S.S.), Newton-Raphson (N.R.), Modified Newton (M.N.), Quasi-Newton (Q.N.) and a segregated (SEGREGATED) solution algorithm. The choice of the solution method depends on the type of problem. A combination of these methods is also possible. The aim is to achieve converged solution with less number of iterations and less time. The current problem is solved using S.S. method and SEGREGATED algorithm.

CHAPTER 6

RESULTS AND CONCLUSIONS

The results of the analysis is shown in a number of plots. The characteristics of the high velocity waterjet and abrasive stream are illustrated in figures 6.1-6.6.

6.1 Velocity Distribution

One of the primary objectives of the analysis was to investigate the acceleration of abrasive particles in the abrasive jet. The distribution of velocity vector along the jet is shown in figure 6.1.

The initial velocity of the high velocity jet is constant and equal to 700 m/sec. at the inlet port. This velocity is taken as the reference velocity and the velocity distribution along the jet is plotted as fraction of the reference velocity. Even though the flow is essentially turbulent, the presence of the thin laminar sub layer at the boundary of the wall changes the distribution of velocity. At the exit of the sapphire, the velocity distribution is approximately parabolic. It is interesting to note that the velocity increases along the axial line up to the exit region and then decreases. Figure 6.2 shows the velocity along the axis of the jet. The peak point in the graph corresponds to the exit point of the sapphire. The increase in velocity is about 1.34 at this point.

At the exit of the sapphire, the waterjet meet the abrasive stream from the annular slit of the nozzle. The velocity of the abrasive stream is taken as 2 m.sec. The layer close to the waterjet gains momentum from the high velocity jet and gets accelerated. As the flow continue, there is a transfer of energy from high velocity jet to the low velocity stream. This transfer continues along the successive layers in the radially outward direction. As the law of conservation of momentum necessitates, the waterjet in the core region looses the energy and the outer region gains acceleration as the flow proceeds.

Figure 6.3 represents the velocity distribution across the jet at various stand off distances. At 5 mm stand off distance, the velocity at the core is about 1.25. Along successive sections, the velocity decreases at the core, and increases at the periphery.

Figure 6.4 shows the distribution of velocity contour. Points of same velocity are connected by line. This also another way of representing the velocity distribution.

6.2 Mixing Characteristics

In an AWJ system, the function of the water jet is to accelerate the abrasive particles to enable the cutting action. Hence for effective cutting, there has to be sufficient concentration of abrasive particles at the core where the velocity is maximum.

By tracing the path of individual points in the jet, the nature of mixing can be studied. The numerical method used for modeling the abrasive jet is capable of displaying the position of individual points at specified time intervals. The line connecting all these positions is the trajectory of the particle present at the initial point.

Figure 6.5 illustrates the particle path plot. Since the objective is to study the mixing of abrasives, a typical point in the abrasive stream is chosen for the plot. This point represents a single abrasive particle. The initial position of the point is inside the annular slit where the abrasive particle has low velocity. As shown in the figure, the trajectory is parallel to the axis. From the velocity contour plot (figure 6.4) it can be seen that the trajectory is within the zone that has velocity greater than 0.6.

Figure 6.6 is a streamline contour plot of the jet. The flow pattern of various layers shown in this plot.

Although it is not clear whether the abrasive particles can reach very close to the axis of the jet, the fact that abrasives reach the higher velocity zone demonstrate the mixing capability of the AWJ system.

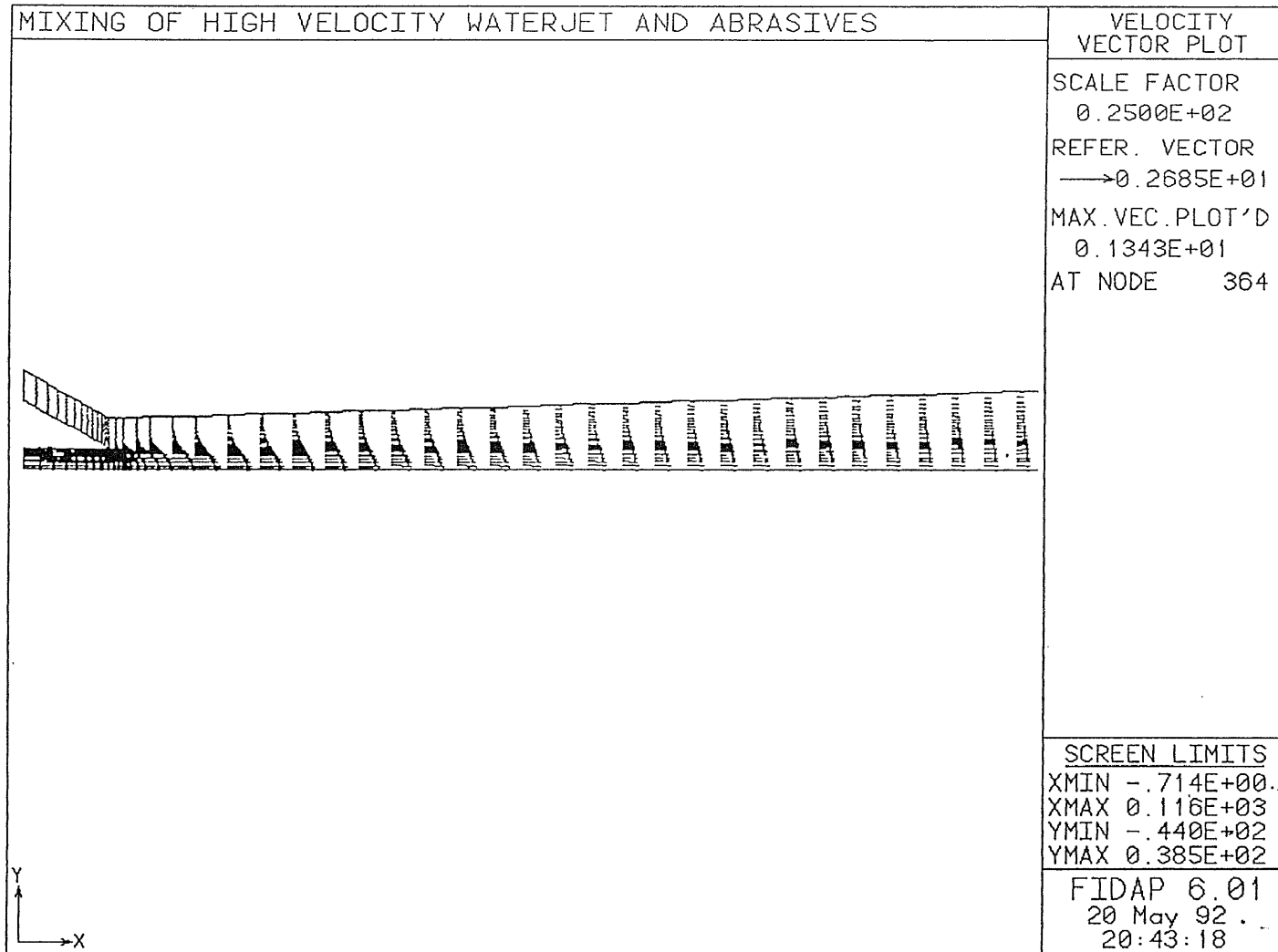


Figure 6.1 Velocity Vector Plot

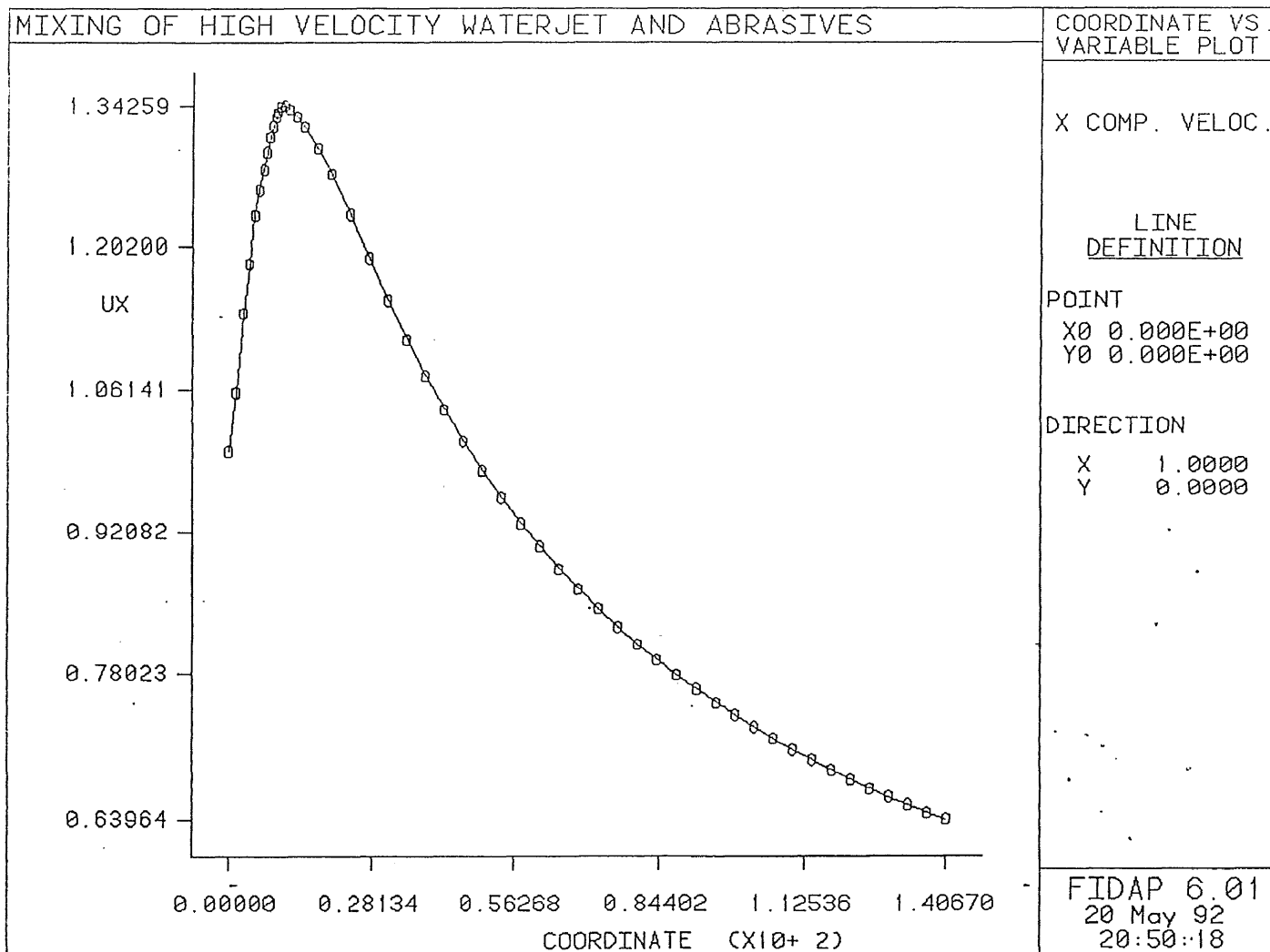


Figure 6.2 Velocity of a Particle Moving Along the Axis of the Jet

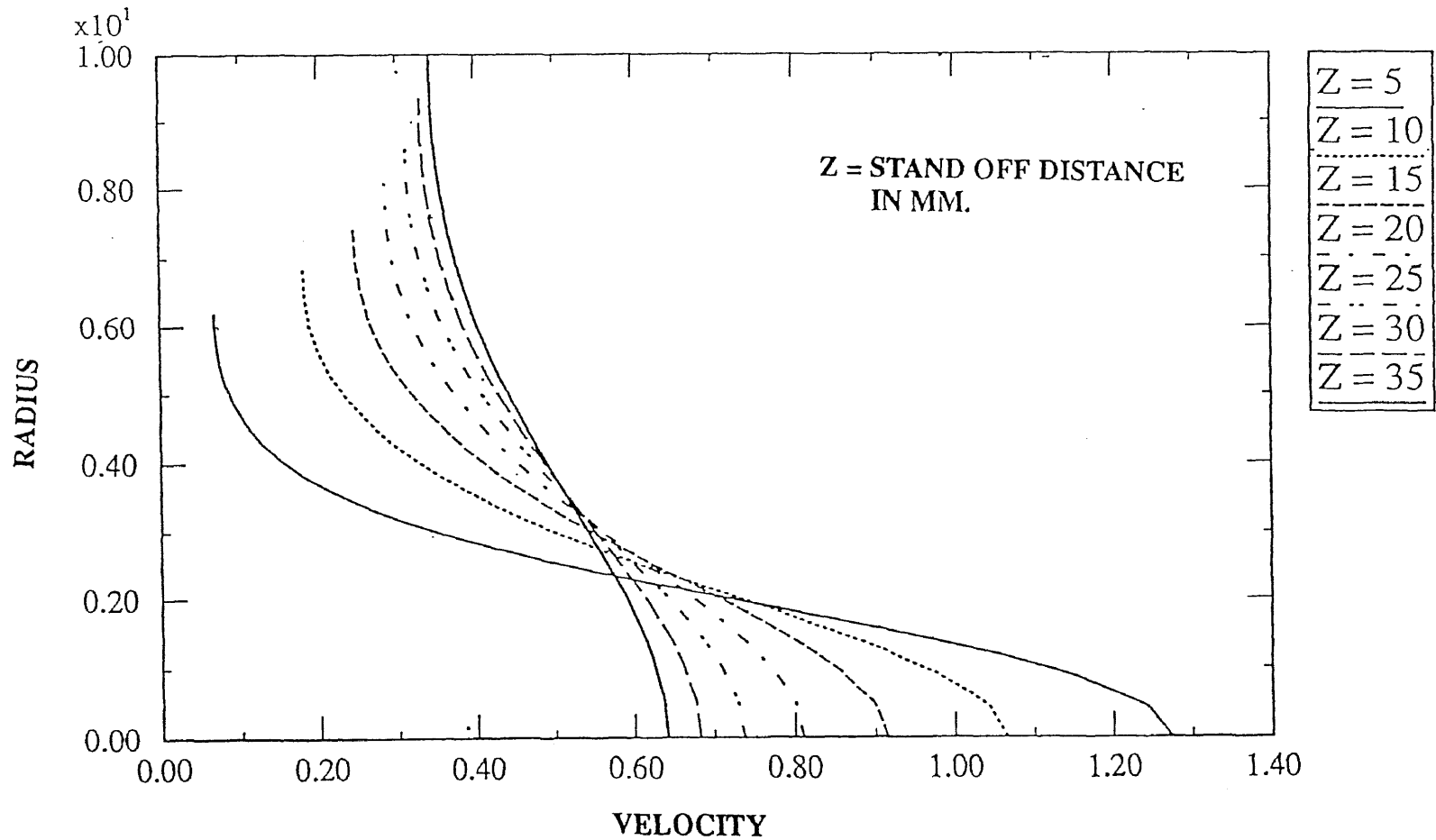


Figure 6.3 Velocity Profile of the Abrasive Jet at Various Stand off distances

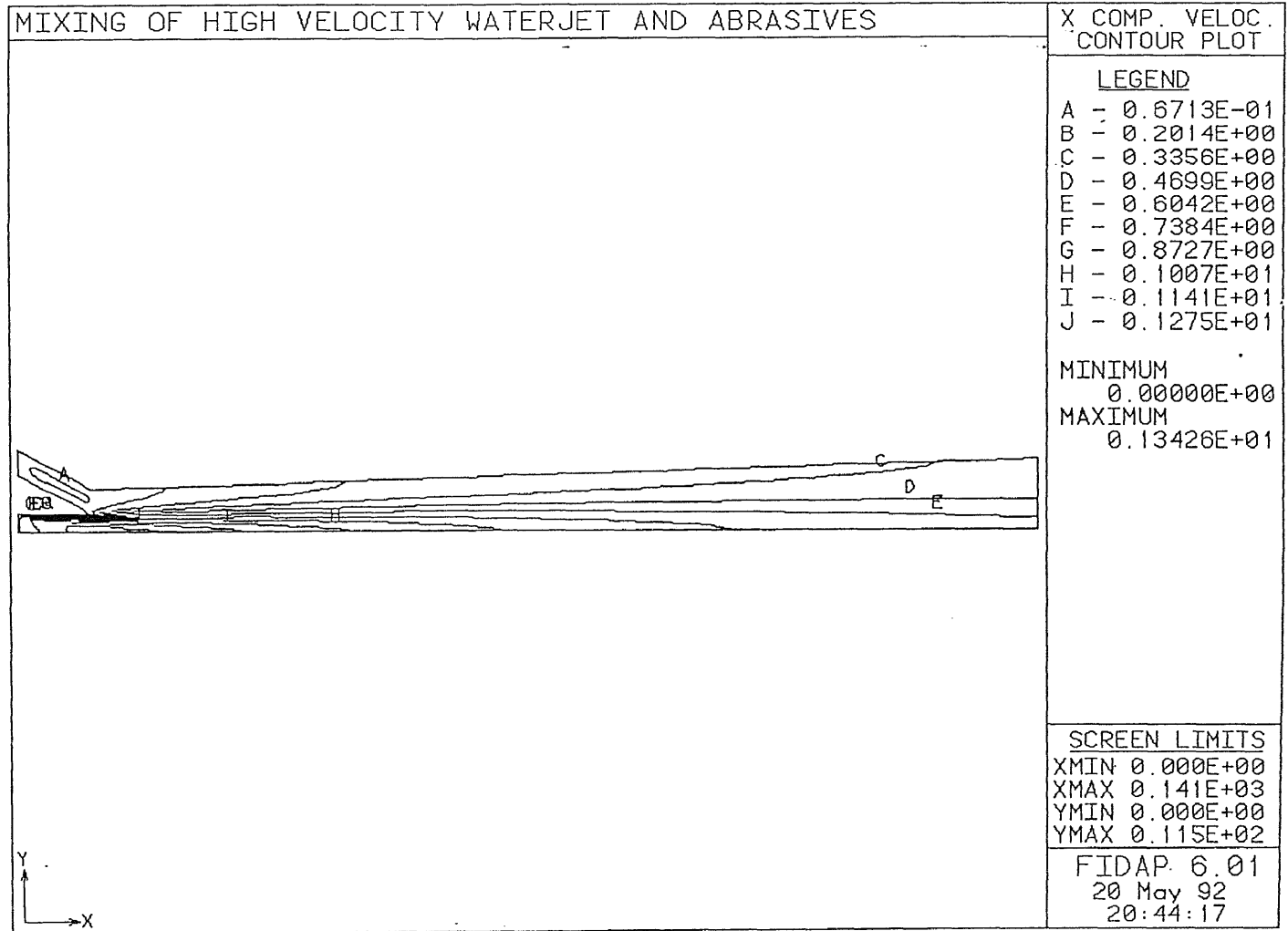


Figure 6.4 Velocity Contour Plot.

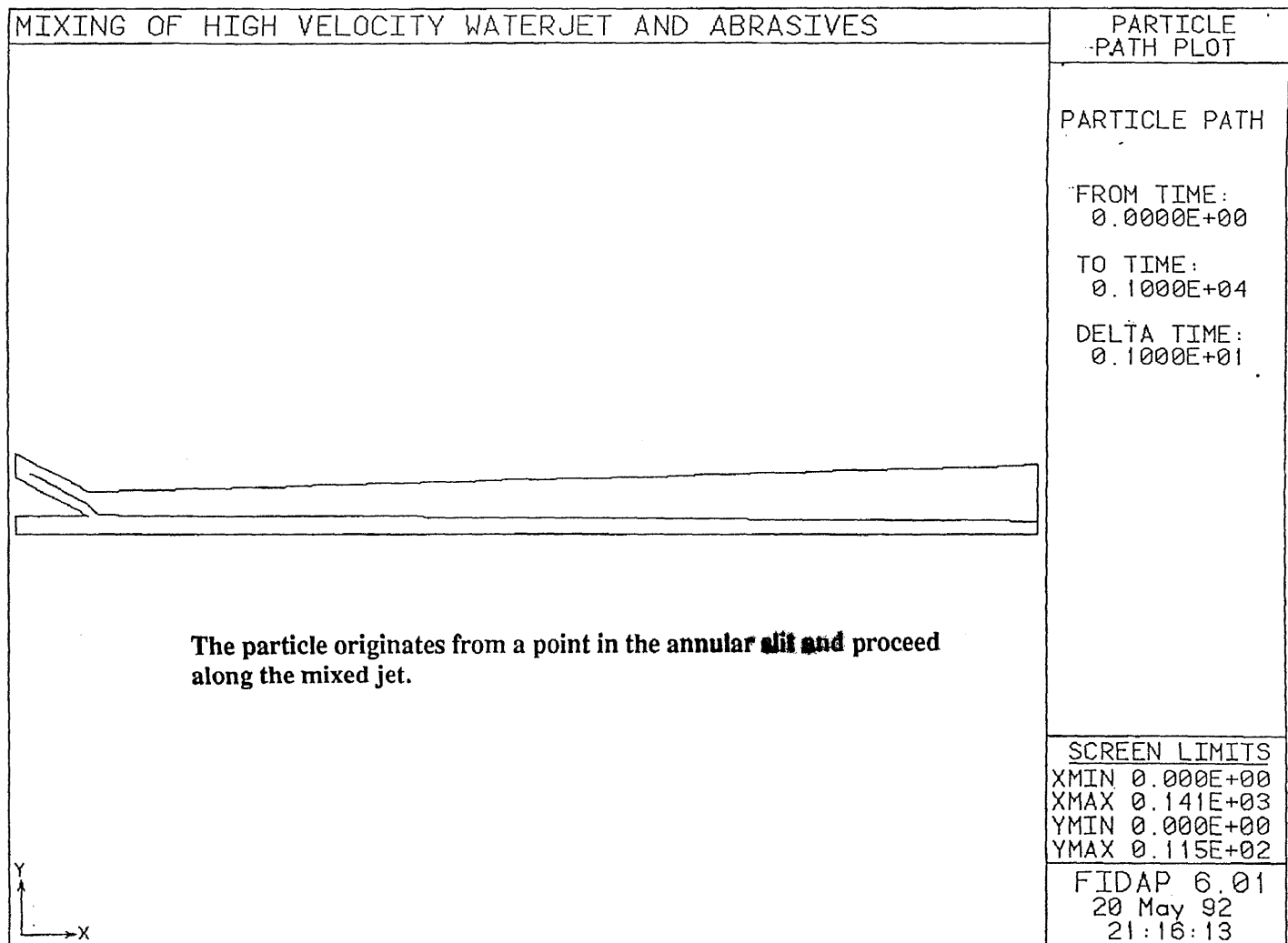


Figure 6.5 Trajectory of a Typical Particle in the Abrasive Stream .

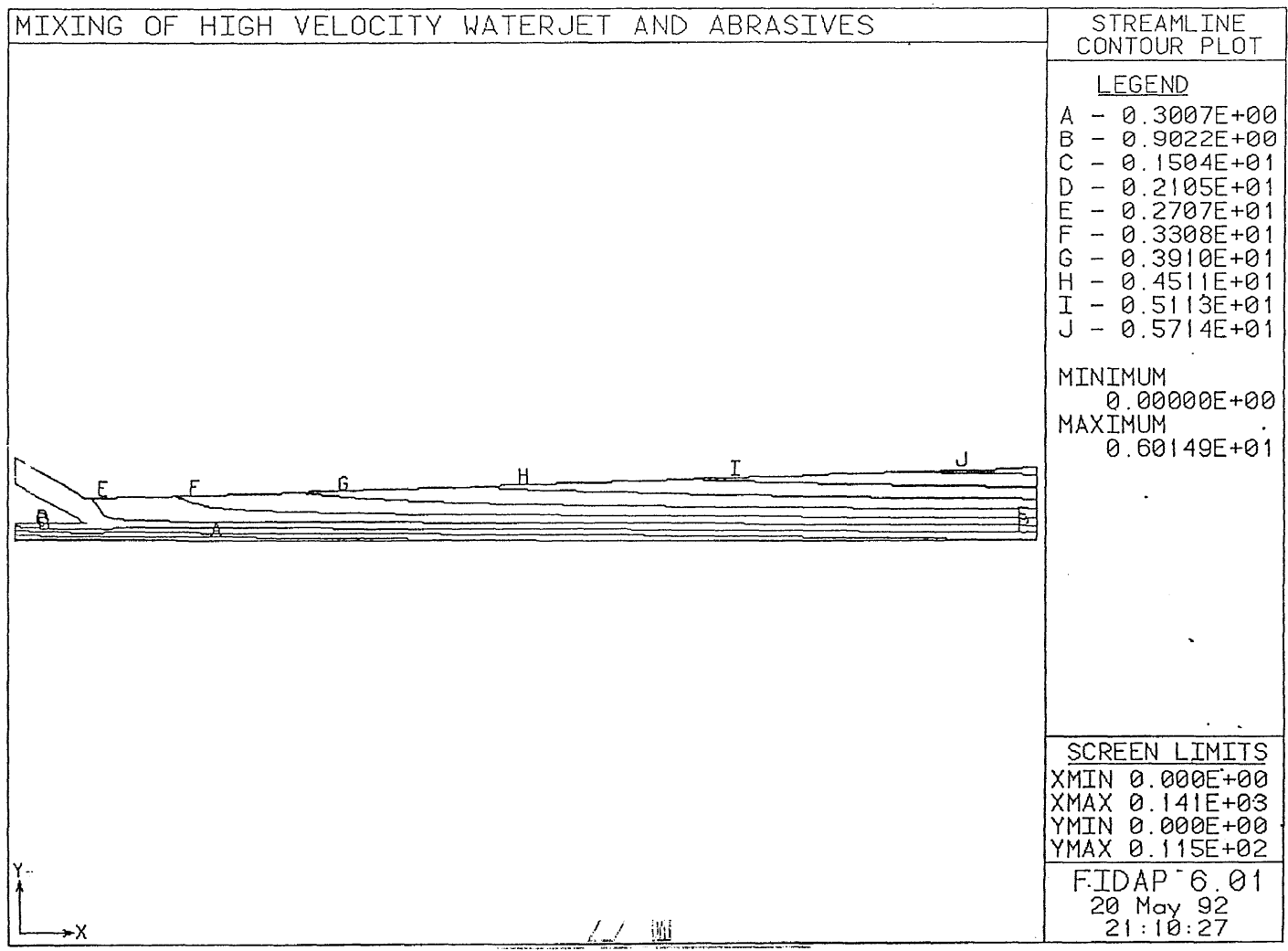


Figure 6.6 Streamline Contour Plot.

APPENDIX B

FIDAP INPUT FILE FOR INITIAL SOLUTION

```
*NOINTERACTIVE
*TITLE
MERGING HIGH VELOCITY JET AND ABRASIVE SLURRY
*FIMESH(2-D,IMAX=5,JMAX=6)
EXPI
/1 2 3 4 5
1 0 13 0 51
EXPJ
/1 2 3 4 5 6
1 0 13 14 0 28
POINT(CARTESIAN)
1 1 1 1 0.0 0.
2 3 1 1 10. 0.
3 5 1 1 140.67 0.
4 5 3 1 140.67 2.5
5 3 3 1 10. 2.5
6 1 3 1 0.0 2.5
7 1 4 1 0.0 8.
8 3 4 1 10. 2.5
9 5 4 1 140.67 2.5
10 5 6 1 140.67 6.
11 3 6 1 10. 6.
12 1 6 1 0.0 11.5
LINE
1 2 4. 4
2 3 4. 3
3 4 5. 4
5 4 4. 3
6 5 4. 4
1 6 6. 4
2 5 7. 4
7 8 4. 4
8 9 4. 3
9 10 3. 3
11 10 4. 3
12 11 4. 4
7 12 2. 3
8 11 2. 3
SURFACE
1 5
```

```
2 4
7 11
8 10
MERGE
8 9 5 4
ELEMENTS(QUADRILATERAL,NODES=9)
1 4
7 10
ELEMENTS(BOUNDARY,NODES=3)
10 11
4 5
BCNODE(UX)
6 5 0.
7 8 0.
12 11 0.
11 10 0.
BCNODE(UY)
1 2 0.
1 6 0.
6 5 0.
7 8 0.
12 11 0.
11 10 0.
BCNODE(UX)
1 6 1.
7 12 .05
BCNODE(UY)
7 12 -.02
BCNODE(SURFACE)
11 10
5 5 1.
8 8 1.
/BCNODE(KINETIC)
1 6 0.001
7 12 0.001
BCNODE(DISSIPATION)
1 6 4.5E-4
7 12 4.5E-4
NUMBER
2 1
SPINES
11 2 10 0.
END
*FIPREP
/PROBLEM(NONLINEAR,AXI-SYMMETRIC,STEADY,TURBULENT)
```

```
PRESSURE(MIXED=1.E-7,DISCONTINUOUS)
EXECUTION(NEWJOB)
/SOLUTION(S.S.=20,VELCONV=.01,RESCONV=.02,ACCF=0.5)
OPTIONS(STRESSDIVERGRNCE)
NODES(FIMESH)
/ICNODE(KINETIC, CONSTANT=0.001)
/ICNODE(DISSIPATION,CONSTANT=4.5E-4)
/ICNODE(VELOCITY,READ)
VISCOSITY(SET=1,K.E.)
5.198E-6
VISCOSITY(SET=2,K.E.)
5.198E-6
SURFACETENSION(SET=1,CONSTANT=0.,ANG1=0.,ANG2=180.)
SURFACETENSION(SET=2,CONSTANT=2.,ANG1=0.,ANG2=180.)
ELEMENTS(QUADRILATERAL,NODES=9,FIMESH,MVISC=2)
ELEMENTS(QUADRILATERAL,NODES=9,FIMESH,MVISC=1)
ELEMENTS(WALL,NODES=3,FIMESH)
ELEMENTS(WALL,NODES=3,FIMESH)
ELEMENTS(WALL,NODES=3,FIMESH)
ELEMENTS(SLIP,NODES=3,FIMESH,MSURF=2)
ELEMENTS(SLIP,NODES=3,FIMESH,MSURF=1)
/ELEMENTS(SURFACE,NODES=3,FIMESH,MSURF=2)
/ELEMENTS(SURFACE,NODES=3,FIMESH,MSURF=1)
RENUMBER
END
*END
```

APPENDIX C

FIDAP INPUT FILE FOR FINAL SOLUTION

```
*NOINTERACTIVE
*TITLE
MERGING HIGH VELOCITY JET AND ABRASIVE SLURRY
*FIMESH(2-D,IMAX=5,JMAX=6)
EXPI
/1 2 3 4 5
1 0 13 0 51
EXPJ
/1 2 3 4 5 6
1 0 13 14 0 28
POINT(CARTESIAN)
1 1 1 1 0.0 0.
2 3 1 1 10. 0.
3 5 1 1 140.67 0.
4 5 3 1 140.67 2.5
5 3 3 1 10. 2.5
6 1 3 1 0.0 2.5
7 1 4 1 0.0 8.
8 3 4 1 10. 2.5
9 5 4 1 140.67 2.5
10 5 6 1 140.67 6.
11 3 6 1 10. 6.
12 1 6 1 0.0 11.5
LINE
1 2 4. 4
2 3 4. 3
3 4 5. 4
5 4 4. 3
6 5 4. 4
1 6 6. 4
2 5 7. 4
7 8 4. 4
8 9 4. 3
9 10 3. 3
11 10 4. 3
12 11 4. 4
7 12 2. 3
8 11 2. 3
SURFACE
1 5
```



```
2 4
7 11
8 10
MERGE
8 9 5 4
ELEMENTS(QUADRILATERAL,NODES=9)
1 4
7 10
ELEMENTS(BOUNDARY,NODES=3)
10 11
4 5
BCNODE(UX)
6 5 0.
7 8 0.
12 11 0.
/11 10 0.
BCNODE(UY)
1 2 0.
1 6 0.
6 5 0.
7 8 0.
12 11 0.
/11 10 0.
BCNODE(UX)
1 6 1.
7 12 .05
BCNODE(UY)
7 12 -.02
BCNODE(SURFACE)
11 10
5 5 1.
8 8 1.
BCNODE(KINETIC)
1 6 0.001
7 12 0.001
BCNODE(DISSIPATION)
1 6 4.5E-4
7 12 4.5E-4
NUMBER
2 1
SPINES
11 2 10 0.
END
*FIPREP
PROBLEM(NONLINEAR,AXI-SYMMETRIC,STEADY,TURBULENT,FREE)
```

```
PRESSURE(MIXED=1.E-7,DISCONTINUOUS)
EXECUTION(NEWJOB)
/SOLUTION(S.S.=20,VELCONV=.01,RESCONV=.02,ACCF=0.5)
OPTIONS(STRESSDIVERGRNCE)
NODES(FIMESH)
ICNODE(KINETIC, CONSTANT=0.001)
ICNODE(DISSIPATION,CONSTANT=4.5E-4)
ICNODE(VELOCITY,READ)
VISCOSITY(SET=1,K.E.)
5.198E-6
VISCOSITY(SET=2,K.E.)
5.198E-6
SURFACETENSION(SET=1,CONSTANT=0.,ANG1=0.,ANG2=180.)
SURFACETENSION(SET=2,CONSTANT=2.,ANG1=0.,ANG2=180.)
ELEMENTS(QUADRILATERAL,NODES=9,FIMESH,MVISC=2)
ELEMENTS(QUADRILATERAL,NODES=9,FIMESH,MVISC=1)
ELEMENTS(WALL,NODES=3,FIMESH)
ELEMENTS(WALL,NODES=3,FIMESH)
ELEMENTS(WALL,NODES=3,FIMESH)
/ELEMENTS(SLIP,NODES=3,FIMESH,MSURF=2)
/ELEMENTS(SLIP,NODES=3,FIMESH,MSURF=1)
ELEMENTS(SURFACE,NODES=3,FIMESH,MSURF=2)
ELEMENTS(SURFACE,NODES=3,FIMESH,MSURF=1)
RENUMBER
END
*END
```

REFERENCES

- Ayers, G. W. 1987. "Principles of Waterjet Cutting." *Tappi Journal*. September. 91-93.
- Behringer-Ploskonka, C. A. 1987. "Water jet Cutting- a Technology Afloat on a Sea of Potential." *Manufacturing Engineering*. November. 37-41.
- Easton, N. 1978. "Wet Abrasion Blasting." *U. S. Patent Number 4,125,969*. November.
- Griffiths, N. J., and R. G. Godding. 1982. "A preliminary investigation into abrasive water jet cutting of cast iron." *BHRA Fluid Engineering*. December.
- Hart, B. E. 1976. "Guns for forming jets of particulate material." *U. S. Patent Number 3,972,150*. August.
- Hashish, M. 1982. "Steel Cutting with Abrasive Waterjets." *6th International Symposium on Jet Cutting Technology*. April.
- , 1989. "An Investigation of Milling with Abrasive Waterjets." *J. of Engineering for Industry*. May. 111: 158-166.
- , 1990. "Abrasive - fluidjet machining systems: Entrainment versus direct pumping." *10th International Symposium on Jet Cutting Technology*. October. 214-128.
- , 1991. "Optimization factors in abrasive waterjet machining." *J. of Engineering for Industry*. February. 113: 29-37.
- , 1991. "Characteristics of surfaces machined with abrasive waterjets." *J. of Engineering Materials and Technology*. July. 113: 354-362.
- Hashish, M., J. Kirby, and Yih-Ho Pao. 1987. "Method and Apparatus for Forming a High Velocity Liquid Abrasive Jet." *U. S. Patent Number 4,648,215*. March.
- Horii, K., Y. Matsumae, X. Cheng, M. Takei, B. Hashimoto, and T. J. Kim. 1990. "Development of a new mixing nozzle assembly for high pressure abrasive waterjet applications." *10th International Symposium on Jet Cutting Technology*. October. 163-184.
- Hows, John. 1991. "Water jetting on subsea welds." *Offshore*. March. 51: 102.
- Kovacevic, R., and M. Evizi. 1990. "Nozzle wear detection in AWJ systems." *Material Evaluation*. March. 48: 348-353.

- Kusabiraki, D., H. Niki, and K. Yamagiwa. 1990. "Gas entrainment rate and flow pattern of vertical plunging liquid jets." *The Canadian Journal of Chemical Engineering*. December. 68: 893-903.
- Labus, T.J., K. F. Neusen, D. G. Albert., and T. J. Gores. 1989. "Factors influencing abrasive mixing process." *Proc. 5th American Waterjet Conference*. Toronto.
- Maasberg, W., and K. Sparkel. 1969. "Sand blasting apparatus." *U. S. Patent Number 3,424,286*. January.
- Mazurkiewicz, M., Z. Kubala, and J. Chow. 1989. "Metal machining with high pressure waterjet cooling assistance -- a new possibility." *J. of Engineering for Industry*. February. 111: 7-12.
- Mazurkiewicz, M., and G. Galecki. 1990. "Energy Consumed for hydro-abrasive jet formation." *International Journal of Waterjet Technology*. March.
- McCarty, L. H. 1987. "Unusual valve directs powerful water jet." *Design News*. March. 43: 108-110.
- Park, W. J., and J. M. Cimbala. 1991. "The effect of jet injection geometry on two-dimensional momentumless wakes." *J. of Fluid Mechanics*. March. 224: 29-47.
- Saunders, D. H. "Water / Abrasive cutting of slate." 1981. Confidential report CR 1677 *BHRA Fluid Engineering*. March..
- Simpson, Michael. 1990. "Abrasive particle study in high pressure waterjet cutting." *International Journal of Waterjet Technology*. March. 17-28.
- Taylor, C. D., and E. D. Thimons. 1989. "Water-jet-assist improves shearer performance." *Engineering and Mining Journal*. April. 190: 37-39.
- Vijay, M.M. 1990. "Recent advances in the field of High speed waterjets: A review of the 5th American Waterjet Conference." *International Journal of Waterjet Technology*. March. 29-35.
- Wallace, R. B., and S. J. Wright. 1984. "Spreading layer of a two-dimensional buoyant jet." *J. of Hydraulic Engineering*. June. 110: 813-828.
- Watson, J. D. 1978. "Fluid-Abrasive nozzle device." *U. S. Patent Number 4,080,762*. March.
- Woodson, J. P. 1988. "Fundamentals of wet abrasive blasting." *Materials Performance*. October. 27: 31-34.